Journal Pre-proofs

Research paper

Formulation and dermal delivery of a new active pharmaceutical ingredient in an *in vitro* wound model for the treatment of chronic ulcers

Ursula Thormann, Selina Marti, Elizabeth Lensmith, Michael Lanz, Susanne Herzig, Reto Naef, Georgios Imanidis

PII: S0939-6411(24)00199-1
DOI: https://doi.org/10.1016/j.ejpb.2024.114373
Reference: EJPB 114373

To appear in: *European Journal of Pharmaceutics and Biopharmaceutics*

Received Date: 16 February 2024
Revised Date: 4 June 2024
Accepted Date: 16 June 2024

Please cite this article as: U. Thormann, S. Marti, E. Lensmith, M. Lanz, S. Herzig, R. Naef, G. Imanidis, Formulation and dermal delivery of a new active pharmaceutical ingredient in an *in vitro* wound model for the treatment of chronic ulcers, *European Journal of Pharmaceutics and Biopharmaceutics* (2024), doi: https://doi.org/10.1016/j.ejpb.2024.114373

Formulation and dermal delivery of a new active pharmaceutical ingredient in an *in vitro* wound model for the treatment of chronic ulcers

Ursula Thormann[1], Selina Marti[1], Elizabeth Lensmith[1], Michael Lanz[1], Susanne Herzig[1], Reto Naef[2], Georgios Imanidis[1,*]

[1]School of Life Sciences, University of Applied Sciences Northwestern Switzerland, Muttenz/Basel, Switzerland

[2]Topadur Pharma AG, Schlieren, Switzerland

*Correspondence

Institute of Pharmaceutical Technology, School of Life Sciences–FHNW, Hofackerstrasse 30, 4132 Muttenz, Switzerland

georgios.imanidis@unibas.ch

ABSTRACT

The aim of this study was to investigate dermal delivery of the new active pharmaceutical ingredient (API) TOP-N53 into diabetic foot ulcer using an *in vitro* wound model consisting of pig ear dermis and elucidate the impact of drug formulation and wound dressing taking into consideration clinical relevance and possible bacterial infection. Different formulation approaches for the poorly water-soluble API including colloidal solubilization, drug micro-suspension and cosolvent addition were investigated; moreover, the effect of (micro-)viscosity of hydrogels on delivery was assessed. Addition of Transcutol® P as cosolvent to water improved solubility and was significantly superior to all other approaches providing a sustained three-day delivery that reached therapeutic drug levels in the tissue. Solubilization in micelles or liposomes, on the contrary, did not boost delivery while micro-suspensions exhibited sedimentation on the tissue surface. Microbial contamination was responsible for considerable metabolism of the drug leading to tissue penetration of metabolites which may be relevant for therapeutic effect. Use of hydrogels as primary wound dressing under semi-occlusive conditions significantly reduced drug delivery in a viscosity-dependent fashion. Micro-rheologic analysis of the gels using diffusive wave spectroscopy confirmed the restricted diffusion of drug particles in the gel lattice which correlated with the obtained tissue delivery results. Hence, the advantages of hydrogel dressings from the applicatory characteristic point of view must be weighed against their adverse effect on drug delivery. The employed *in vitro* wound model was useful for the assessment of drug delivery and the development of a drug therapy concept for chronic diabetic foot ulcer in the home care setting. Mechanistic insights about formulation and dressing performance may be applied to drug delivery in other skin conditions such as digital ulcer.

KEYWORDS

in vitro wound model, bacterial infection, diabetic foot ulcer, TOP-N53, colloidal formulation, suspension formulation, solubility, (micro-)viscosity, diffusive wave spectroscopy, dermal delivery

1 INTRODUCTION

Diabetes is one of the fastest growing global health emergencies of the 21st century. In 2021, estimated 537 million people aged 20 – 79 years were living with diabetes which corresponds to 10.5% of the world population and is predicted to rise to 783 million by 2054 [1]. A common and one of the most serious complications of diabetes is the diabetic foot ulcer [2]. The life-time risk of developing an ulcer as a diabetic patient ranges between 15 and 25% and is often a common cause of hospitalization [3]. It is a major risk factor for lower extremity amputation because of infected and non-healing foot ulcers [4]. In fact, infection is responsible for 60% of those amputation [3] and generally, the lower limb amputation rates are 10 – 20 times higher among people with diabetes [4]. In the United States the costs of the management of diabetic foot ulcers are between $9 - $13 billion [5].

Diabetes leads to neuropathy and peripheral vascular disease resulting in impaired wound healing. The reduced microcirculation accompanied by endothelial dysfunction and the impaired angiogenesis play an important role in the slow wound healing process of diabetic foot ulcers [3]. The endothelial dysfunction results in diminished production and bioavailability of nitric oxide (NO). This leads to low intracellular cGMP (cyclic guanosine monophosphate) level resulting in reduced microcirculation and angiogenesis [3]. Consequently, the increase in cGMP level is a promising therapeutic strategy for diabetic wound treatment. Topadur Pharma AG developed TOP-N53 a new active pharmaceutical ingredient (API) with dual action mechanism which is metabolized to the two active metabolites, NO and TOP-52 (see Figure 1). NO activates the soluble guanylate cyclase (sGC) which transforms guanosine triphosphate to cGMP. TOP-52 inhibits phosphodiesterase 5 (PDE5) that is responsible for the intracellular degradation of cGMP [6]. Both mechanisms result in increased cGMP levels. NO formation and elevated cGMP levels were observed *in-vitro* and a positive effect on re-epithelization and granulation tissue formation, including angiogenesis was seen in diabetic mice *in vivo* with TOP-N53 [7]. TOP-N53 is thus a promising candidate for the treatment of non-healing diabetic ulcers of Wagner grade 1 entailing superficial ulcers without penetration into deeper layers [8].

The disruption of the skin bears the risk of infections and microbial wound colonization. Chronic wounds have a high polymicrobial burden prone to form a biofilm often composed of *Staphylococcus, Pseudomonas* and *Corynebacterium*[3]. Drug metabolism by microbes on the skin is still poorly understood. Nevertheless, it has been receiving increased attention and an artificial intelligence approach to predict healthy skin microbiome-mediated metabolism of biotics and xenobiotics was recently proposed [9-11].

The standard therapy of diabetic foot ulcers is wound care with extensive and regular debridement and infection control followed by dressings that maintain a moist wound environment to promote epithelialization. Additionally, pressure off-loading is of vital importance, together with preservation of adequate blood flow [2]. For clinicians, choice of a dressing to provide hydration if the wound is dry or absorb fluid if the wound produces excessive exudate is pivotal [3]. Many dressings are available on the market [12-16]. Hydrogels are commonly used in dry as well as wet wounds. They have high water content and exist as low and high viscosity products such as Hydrosorb® Gel (Paul Hartmann AG) and Intrasite® Gel (Smith & Nephew AG), respectively. Hydrogels can hydrate wounds as well as take up some exudate and further facilitate autolytic debridement by loosening slough and necrotic wound debris. They require, however, a secondary dressing to protect the wound, for example a gauze or the hydrofiber AQUACEL® Extra (ConvaTec Inc.) to cover and a transparent adhesive foil such as the semi-permeable membrane Hydrofilm® (Paul Hartmann AG) to close the wound. Semi-permeable membranes are useful as they are not fully occlusive and allow water vapor and gas permeation. Usually, dressings are changed every three days in a home care setting [3, 17].

An additive effect on wound healing when the hydrogel is combined with an active compound was shown by data meta-analysis [18]. Currently the only such commercial hydrogel approved to treat diabetic foot ulcer (REGRANEX by Smith & Nephew AG) contains the platelet-derived growth factor

(PDGF) becaplermin and was shown to promote wound healing better than control but has been issued a black box warning by FDA [3, 19]. Other growth factors and gene therapies encoding growth factors as well as further active pharmaceutical ingredients such as angiotensin analogues, neuropeptides or cytokine inhibitors have been discussed in the literature as promising therapeutic agents for wound treatment [2, 3, 20] but to the best of the authors' knowledge none has received market authorization so far.

Drug delivery into and through intact skin is commonly studied *in vitro* in a diffusion apparatus such as a Franz diffusion cell using a skin biopsy in line with the OECD 428 guideline [21-23] and porcine ear skin is often used as it resembles human skin [24, 25]. In the 1990s the need of permeation assays to evaluate drug delivery in wounds was put forward [26]. Walker et al. were the first to address this topic and evaluated an animal model to mimic ulcerated tissue. They compared human skin (including peri-ulcer and ulcerated tissue) derived from lower limb amputation of diabetic patients, porcine skin from three anatomical sites (ear, abdomen, dorsum), ischemic skin (porcine and guinea pig), and porcine wounds using both whole skin and dermal membrane. They concluded that dermal porcine membrane (abdominal and dorsal) obtained by heat separation of full thickness skin is a representative model to investigate topical drug delivery to wound tissue [27]. Other *in vitro* models simulated compromised or damaged skin by removing the stratum corneum using tape stripping [28-33], these however, do not adequately reflect wound tissue, whereas barrier function decrease in the order of full thickness skin, tape stripped skin, and heat separated dermis has been demonstrated by electrical resistance, tritiated water flux and trans-epidermal-water loss measurements [31]. Finally, *in vitro* models to investigate the biofilm of clinically relevant bacteria were proposed [34] yet no *in vitro* model for drug delivery studies that takes into account opportunistic infection by microbial colonization of the wound exists to the best of the authors' knowledge.

To improve drug delivery of poorly water-soluble drug substances formulated in aqueous vehicles, solubilization by encapsulation of the drug into micelles or liposomes has been employed [35-37]. Another approach involves adding a water-miscible cosolvent to the formulation to increase drug solubility. Transcutol is the commercial name of such a cosolvent that is the highly purified form of diethylene glycol monoethyl ether (DEGEE). It has a well-established safety profile and is approved for various routes of administration, formulations containing up to 49.91% (w/w) of Transcutol are included in the FDA list for dermal application [38, 39]. Transcutol's superior solubilization power outperforms propylene glycol and ethanol making it an interesting pharmaceutical excipient [38]. As Transcutol is reported to diffuse into and through whole skin, it can also improve solubility of the drug within the tissue especially the stratum corneum, eliciting increased permeation [38].

Hydrogels typically used as primary dressings for wound treatment as well as other topically applied pharmaceuticals have an elevated viscosity to improve applicatory characteristics. However, an inverse relationship between viscosity and drug release and/or skin permeation *in vitro* has been reported [40-43]. In some studies, viscoelastic properties of the formulation were found to better correlate with drug permeation and/or release *in vitro* [42, 43]. Nevertheless, such a correlation was not always observed [44] or the results were inconclusive. Ji et al. for example found that the release rate of the growth factor (rhVEGF) was constant over a wide range of bulk viscosities [45]. The microviscosity of the system was invoked in that work to better explain drug release which was in accord with findings that the diffusion coefficient of different salicylates in hydrogels correlated with microviscosity [46]. Hence, microviscosity rather than macroscopic viscosity of gels has been suggested to be a proper predictor of drug release [47-50]. The effect of viscosity to slow down drug release from hydrogels was also clear when the drug was present in a suspended form within the formulation [51, 52].

The overall aim of this study was to investigate the delivery of the new drug substance TOP-N53 into ulcerated skin tissue with an *in vitro* wound model in the presence of opportunistic microbial infection and develop a formulation for constant drug delivery over a three-day period that would be appropriate for clinical treatment of diabetic foot ulcers in a home care setting. This entailed firstly, developing the

in vitro model to simulate the loss of epidermis in Wagner grade 1 ulcers using heat separated pig ear dermis and secondly, elucidating the role of microbes on TOP-N53 metabolism and delivery; thirdly, studying different formulation approaches including solubilization, micro-particle suspension and use of cosolvent with respect to skin delivery of poorly water-soluble TOP-N53 and fourthly, assessing the effect of the viscosity of gel formulations on TOP-N53 delivery under conditions closely mimicking clinical setting; finally, using rheological measurements by diffusive wave spectroscopy for reaching a better understanding of the role of microviscosity on drug delivery rate. The learnings from this study should be applicable to the treatment of other skin conditions such as digital ulcer.

2 MATERIALS & METHODS

2.1 Materials

The compounds TOP-N53 and TOP-52 were kindly provided by Topadur Pharma AG (Schlieren, Switzerland). The phosphate buffered saline (PBS) contained sodium chloride EMPROVE® ESSENTIAL (NaCl, 137 mM), potassium dihydrogen phosphate EMPROVE® bio (KH_2PO_4, 3.5 mM) and di-sodium hydrogen phosphate dehydrate EMPROVE® bio ($Na_2HPO_4 \times 2\ H_2O$, 14 mM) purchased from Merck KGaA (Darmstadt, Germany) and dissolved in purified water. For the preserved PBS, PBS was supplemented with 1% parabens concentrate 10% w/w, made by dissolving methyl parahydroxybenzoate (7% w/w) and propyl parahydroxybenzoate (3% w/w) in propylene glycol at 70°C, both purchased from Hänseler AG (Herisau, Switzerland). Kolliphor® ELP (polyoxyl 35 castor oil) was a gift from BASF (Ludwigshafen am Rhein, Germany), Tween 80 from CRODA (Snaith, UK), Lipoid S 100 from Lipoid GmbH (Ludwigshafen, Germany), Blanose™ 7MF and Blanose™ 7H4XF (sodium carboxymethylcellulose) from Ashland (Wilmington, DE, USA), Vivastar® P (sodium starch glycolate) from JRS (Rosenberg, Germany), Transcutol® P (diethylene glycol monoethyl ether) from Gattefossé (Saint-Priest, France) and benzyl alcohol special grade (benzaldehyde ≤ 0.05%) EMPROVE® EXPERT from Merck KGaA (Darmstadt, Germany). Transcutol® P is referred to in the rest of this paper simply as Transcutol. Super refined® PEG 400-LQ-(MH) (polyethylene gylcol 400) was purchased from CRODA (Snaith, UK), glycerol and potassium carbonate from Hänseler AG (Herisau, Switzerland), and the antibiotic antimycotic solution (100 x) with penicillin (10 000 units/mL), streptomycin (10 mg/mL) and amphotericin B (25 µg/mL) as well as the gentamicin sulfate were obtained from Merck KGaA (Darmstadt, Germany). Acetonitrile and formic acid were bought from Merck KGaA (Darmstadt, Germany) and were of HPLC grade. Water purified by reversed osmosis or ion exchange resin with the water purification system arium® 61215 or arium® pro, respectively, from Sartorius (Goettingen, Germany) was used throughout.

2.2 Formulations

2.2.1 Liquid formulations

Aqueous
Micellar formulation

The micellar formulation was prepared by dissolving Kolliphor ELP (1% w/w) and PEG 400 (10% w/w) in PBS and stirring overnight. Subsequently, a stock solution TOP-N53 in PEG 400 (4 or 10 mM) was added to a final drug concentration of 10 µM and stirred again overnight.

The micellar formulation containing 10 µM TOP-52 was made by dissolving Kolliphor ELP (1% w/w) in PBS (no PEG added), stirring overnight, and subsequently adding a 3.33 mM TOP-52 stock solution in PEG 400 to obtain a final 10 µM TOP-52 concentration and agitated.

Liposomal formulation

Liposomal formulation with 1% w/w Lipoid S 100 was made by dispersing the phospholipid in PBS with a polytron (PT 3100 D, Aggregate N: PT-DA 12/2 EC-F154) for 2 min at 15 000 rpm. The mixture was extruded under nitrogen pressure (max. 8 bar) through polycarbonate filters (Nucleopore track edge membrane filters, Whatman plc, Kent, UK) pore size 0.4 µm (3 times), 0.2 µm (5 times), and 0.1 µm (2 × 10 times). A 10 mM stock solution of TOP-N53 in PEG 400 was added to the liposomes to reach a final drug concentration of 10 µM and stirred overnight.

Suspension formulation

TOP-N53 (2% w/w) was suspended in PBS with Tween 80 (0.5% w/w) and benzyl alcohol (1% w/w) and milled with a stirred media mill (DYNO®-MILL RESEARCH LAB, Willy A. Bachofen, Muttenz, Switzerland) equipped with a 79.6 mL grinding chamber and an accelerator made of steel. 100 mL of TOP-N53 suspension were milled for 60 min at 2 700 rpm with yttria-stabilized zirconia beads (diameter 0.5 mm, YTZ® grinding media, Tosoh Corporation, Tokyo, Japan). The filling ratio of the grinding media was 60% (47.8 mL). The suspension was stored at 4°C and used as stock suspension to prepare all liquid, low viscosity and high viscosity suspension formulations.

The 2% w/w TOP-N53 suspension was diluted with either PBS to obtain a content of 5, 8 or 100 µM TOP-N53, or with PBS containing penicillin/streptomycin/amphotericin B (100 U/mL, 0.1 mg/mL, 0.25 µg/mL, respectively) or gantamicin sulfate (50 mg/mL) to reach a final 100 µM TOP-N53 suspension formulation. The suspension formulations were stirred overnight before the experiments.

Transcutol in water

Solution formulation

The TOP-N53 stock solution in PEG 400 (4 mM) was added to 45% w/w Transcutol in water to a final drug concentration of 10 µM TOP-N53 and stirred well.

Suspension formulation

The 2% TOP-N53 stock suspension (preparation see liquid aqueous suspension formulation) was added to 45% w/w Transcutol in water to reach a final 100 µM TOP-N53 suspension formulation and stirred overnight.

2.2.2 Semisolid formulations

Low viscosity aqueous & 45% Transcutol in water gel formulations

To prepare the 100 µM TOP-N53 low viscosity aqueous gel formulation, Blanose™ 7MF (1.5% w/w) was soaked under stirring in the liquid 100 µM TOP-N53 suspension formulation until the Blanose was dispersed.

For the 100 µM TOP-N53 low viscosity 45% Transcutol in water gel formulation containing Blanose™ 7MF (1.5% w/w), the required amount of 2% TOP-N53 stock suspension was first diluted with water (54.2% w/w). Blanose™ 7MF was then dispersed in the suspension and subsequently Transcutol (44.3% w/w) was added slowly, both under agitation. The final formulation was stirred overnight.

High viscosity aqueous & 45% Transcutol in water gel formulations

The 100 µM TOP-N53 high viscosity aqueous gel formulation consisted of Blanose™ 7H4XF (1% w/w), glycerol (5% w/w), Vivastar® P (5% w/w) and water (89% w/w) and was manufactured in the Mi Molto mixing and homogenizing machine (Krieger AG, Muttenz, Switzerland) equipped with a double walled glass vessel, pressure control, metal propeller and plastic scrapers. Water and glycerol were mixed in

the vessel and the required amount of the 2% TOP-N53 stock suspension was pipetted to the mixture and stirred for 2 min at 50 rpm. Blanose™ 7H4XF was added slowly in portions to the suspension under agitation at 100 rpm and after adding the last portion, the vessel was set under vacuum (20 mbar) and the gel was stirred for a total of roughly 4.5 h until Blanose™ 7H4XF was dispersed. Vivastar® P was added portion-wise, and the gel was stirred for 10 h at 100 rpm under vacuum (20 mbar) to avoid the formation of air bubbles. The vessel was kept at a temperature < 40°C during the whole process. The formulation was stored for 5 days at 4°C prior to the experiment.

The 100 µM TOP-N53 high viscosity 45% Transcutol in water gel formulation consisted of Blanose™ 7H4XF (1.7% w/w), glycerol (5% w/w), Transcutol (42% w/w) and water (51.3% w/w) and was manufactured in the Mi Molto machine. Water and glycerol were mixed in the vessel and the required amount of 2% TOP-N53 stock suspension was pipetted to the mixture and stirred. Subsequently Blanose™ 7H4XF was added portion-wise and was mixed at 100 rpm under vacuum (15 mbar) for a total of 3.6 h until dispersed. Transcutol was added very slowly in small portions and subsequently the gel was stirred for almost 8 h under vacuum (15 mbar). The system was kept at 20 – 25°C during the entire process. The final gel was stored under nitrogen in an exicator containing saturated potassium carbonate solution in water to provide relative humidity of around 44% for 1.5 weeks days prior experiment. The drug content of 100 µM of both high viscosity gel formulations was defined using a final density of 1 g/mL.

2.3 Bioconversion test & *in vitro* transport experiment

2.3.1 Dermis preparation

Freshly slaughtered pig ears were provided by the nearby slaughterhouse. The pigs were not older than 5 months of both genders and not scalded (information from the slaughters). The ears were washed in the lab with tap water and shaved with an animal hair clipper. The full thickness skin of the dorsal site of the ear was removed from the underlying cartilage with a scalpel. The dermis was separated from the epidermis by heat separation. Hereby, the full thickness skin was immersed in a water bath (60°C) for 90 s, and the epidermis was scraped off with a spatula. The dermis was washed with water, wrapped in aluminum foil and stored for no longer than 30 days at -20°C until use.

2.3.2 Franz diffusion cells

The frozen dermis was thawed, cut into pieces, and mounted on custom made Franz diffusion cells. The boundary between donor and acceptor compartment was sealed with Teflon tape (Merck KgaA, Darmstadt, Germany), the acceptor compartment was equipped with a magnetic stirrer bar and the cells were fixed on a suitable metal holder on top of a magnetic stirrer plate and placed in a water bath. For microneedle treatment in selected instances the AdminStamp 600 microneedle array device containing the AdminPatch® Array 600 microneedle array attached to an applicator (187 x 500 µm needles, nanoBioSciences LLC, DBA AdminMed, Sunnyvale, California USA) was applied to the dermis with 2 kg for 10 s before mounting into the cell. The surface area of diffusion of the cells was between 1.78 and 2.20 cm^2. This setting was used for the bioconversion test and the transport experiment.

2.3.3 Bioconversion test

The bioconversion test was carried out with the liquid aqueous suspension formulation with and without addition of antimicrobial agents penicillin/streptomycin/amphotericin B and the liquid 45%

Transcutol in water suspension formulation. The placebo formulations were pre-exposed to dermis in the donor compartment of Franz diffusion cells for 72 h at 28°C under the conditions described below for the transport experiment. Subsequently, 500 µL of the donor solution was put in a 4 mL brown glass vial and 500 µL of the corresponding 100 µM TOP-N53 suspension formulation was added. As a control, placebo formulation which had not been in contact with the tissue was used. The vials were vortexed for 30 s, protected from light with aluminum foil and placed in a water bath at 28°C for 72 h. One hundred µL samples were taken at different time points. The vials were vortexed before each sampling and the samples were pipetted to a 2 mL Eppendorf tube and diluted 1:4 with CH_3CN:H_2O (50:50). Samples were centrifuged for 30 min at 4°C at 16 100 × g (5415R or 5472R, Eppendorf AG, Hamburg, Germany) and analyzed by HPLC-UV-MS.

2.3.4 *In vitro* transport experiment

Firstly, the acceptor compartment was filled with solution (5 – 8 mL) up to a level to avoid hydrostatic water flow. In the experiments with the micellar and liposomal formulation, the placebo formulation was used as acceptor solution. With the liquid suspension formulation, low viscosity aqueous formulation and the TOP-52-containing micellar formulation, a micellar solution with 1% w/w Kolliphor ELP in PBS was used which was supplemented with either antibiotics/fungicide in the respective experiments or with parabens when the liquid or low viscosity 45% Transcutol in water formulations as well as the high viscosity aqueous and Transcutol in water formulations were used. 45% Transcutol in water was applied as acceptor solution in an experiment with the liquid 45% Transcutol in water formulation to test the effect of osmotic pressure difference.

Secondly, the formulations containing TOP-N53 or TOP-52 were added to the donor compartment. The liquid aqueous formulations were added in three different doses. For the low dose, approximately 0.7 mL corresponding to an applied product thickness of approx. 4 mm of the 10 µM TOP-N53 micellar and 5 µM TOP-N53 suspension formulation was used. For the intermediate dose, 4 mL (≈ 20 mm product thickness) of the 10 µM TOP-N53 micellar, 10 µM TOP-N53 liposomal and 8 µM TOP-N53 suspension formulation was added. For the highest dose with the 100 µM TOP-N53 suspension liquid formulation 0.9 – 1 mL (≈ 5 mm product thickness) was applied. The same amount was used for the liquid 45% Transcutol in water formulations with 10 µM and 100 µM TOP-N53, the 100 µM TOP-N53 low and high viscosity aqueous and 45% Transcutol in water formulations and the micellar formulation containing 10 µM TOP-52. One Franz diffusion cell was always run with corresponding placebo formulation in the donor compartment and used as reference in the chromatographic analysis of the samples.

The acceptor compartment was closed with a rubber plug to avoid water evaporation. The formulation in the donor compartment was covered with a semi-permeable membrane (Hydrofilm® roll, IVF Hartmann AG, Neuhausen, Switzerland) except for the low and intermediate dose liquid aqueous formulations for which a rubber plug was used and sealed in the perimeter with Teflon tape. The acceptor solution was magnetically stirred at 500 rpm, the experiment was carried out under light exclusion in a dark room or by aluminum foil wrapping and the water bath was set to 37°C for the low and intermediate dose liquid aqueous formulations and 28°C for all other experiments.

Samples of 100 µL were taken from the acceptor compartment at various time points during 6 – 72 h and replaced with pre-warmed acceptor solution. Dermis tissue was analyzed for drug content at 6, 24, 48 and 72 h by disassembling two Franz diffusion cells at each time point. The donor compartment was first rinsed with CH_3CN:H_2O (50:50) to withdraw remainder formulation, the diffusion cells were disassembled and the tissue and the glass of the donor compartment were washed with CH_3CN:H_2O (50:50). All samples were centrifuged for 30 min at 4°C with 16 100 × g (5415R or 5472R, Eppendorf AG, Hamburg, Germany) before HPLC-UV-MS analysis. The dermis was wrapped in aluminum foil and stored at -20°C prior to extraction.

2.3.5 Dermis extraction

The frozen dermis was cut into pieces with a scalpel and milled with a cryogenic grinder (6770 Freezer/Mill 6770, SPEX® SamplePrepThermo, Metuchen, NJ, USA; Settings: 10 min precool, 4 x 2 min cycles at a rate of 10 counts per seconds). The powder was transferred into a 15 mL Falcon tube, 1.5 mL CH_3CN:H_2O (50:50) was added and vortexed. The powder clump was dispersed with an ultrasonic disintegrator (Branson Sonifier 250, Model 101-063-197, Branson Ultrasonic Corporation, USA; equipped with a tapered microtip, 3.2 mm, for a 13 mm horn; Settings: Output control 2, duty cycles 30% for 60 s). Then, the suspension was shaken with a horizontal shaker (KS15, Edmund Bühler GmbH, Bodelshausen, Germany or KS 3000 i control, IKA®-Werke GmbH & Co. KG, Staufen, Germany) for 3 min at 37°C and centrifuged for 1 h at 25°C with 3 130 × g (5810R, Eppendorf AG, Hamburg, Germany). The supernatant was transferred into a 2 mL Eppendorf tube and centrifuged for 1 h at 25°C with 16 100 × g (5415R or 5472R, Eppendorf AG, Hamburg, Germany). This step was repeated until the supernatant was clear before a final centrifugation for 1 h at 4°C with 16 100 x g. The withdrawn samples were analyzed by HPLC-UV-MS.

2.4 Analytics

2.4.1 Osmolality measurement

Samples were place in a 2 mL Eppendorf tube and osmolality was determined with a freezing point osmometer (Osmomat 010 or Osmomat 3000 , GOMOTEC, Berlin, Germany).

2.4.2 Particle size determination

The particle size of the liquid aqueous micellar and liposomal formulations was measured by dynamic light scattering using a Zetasizer (Nano ZS, Malvern Instruments, Worcestershire, UK). The particle size of the liquid and low viscosity suspension formulations was determined by laser diffractometry (Sympatec, Helios, Clausthal-Zellerfeld, Germany).

2.4.3 Mechanical rheology

The macroscopic rheological properties of low and high viscosity aqueous and 45% Transcutol in water formulations were measured with a Bohlin Gemini rheometer (Malvern Instruments Ltd., Malvern, UK) equipped with a plane – cone geometry (60 mm, 2°, gap: 70 µm) for low viscosity and plane – plane geometry (20 mm, gap: 1 mm) for high viscosity formulations. Both were covered with a solvent trap to prevent evaporation. The rheometer was run in oscillation mode at 28°C. The maximum strain amplitude for staying within the linear elastic response range was determined with an amplitude sweep at 1 Hz. The elastic (G') and the viscous (G'') modulus were measured by a frequency sweep at constant maximum strain amplitude of 0.1 for low viscosity aqueous and 45% Transcutol in water formulations and 0.001 and 0.03 for high viscosity aqueous and 45% Transcutol in water formulations, respectively.

2.4.4 Diffusive wave spectroscopy (DWS)

Experimental setup

To investigate the diffusive behavior of suspended particles and the micro-rheological properties of the liquid, low and high viscosity formulations, diffusive wave spectroscopy (DWS) based on multiple scattering of light by optically turbid samples was applied.

This technique and the used DWS RheoLab (LS Instruments AG, Freiburg, Switzerland) was extensively described previously [53, 54]. Briefly, the instrument was run in transmission mode and the laser light (λ = 685 nm) was scattered by a ground glass and collected before illuminating the sample. The Two-cell Echo Technique was used in which the ground glass rotates producing a periodically changing speckle pattern resulting in an independent statistical ensemble of the intensity function. After passing through the sample the light is detected and the temporal fluctuations of the detected intensity are correlated by a hardware correlator to determine the intensity correlation function. The mean square displacement (MSD) was calculated from the intensity correlation function in a range of lag-times starting at decay ≥ 0.5% and ending at the suggestion of the software by modeling the propagation of light as a diffusive process. The approximation of light propagation by the diffusion equation in sufficiently turbid media is fulfilled only when the optical turbidity of the media L/l* (L = cuvette thickness, l* = transport mean free path, measured by the instrument) is between 5 and 30. Finally, the MSD was related to the Stokes-Einstein relation to obtain the elastic (G') and viscous (G'') modulus [55-59].

Sample preparation & measurement

To obtain sufficient optical turbidity, polystyrene latex tracer particles with a diameter of 310 or 2 200 nm obtained as 10% w/v suspension in water from MAGSPHERE Inc. (Pasadena, CA, USA) were added to placebo formulations. Tracer particles were pipetted to the liquid and the low viscosity formulations under magnetic agitation to obtain a final particle concentration of 1% w/v for all formulations apart from the liquid 45% Transcutol in water formulation with 2 200 nm tracer particles for which a concentration of 2% w/v was used. Water content of the formulations was adjusted for the addition of the tracer particle suspension. The samples were stirred for 10 min and the liquid formulations were immediately filled into quartz cuvettes (LS Instruments AG, Freiburg, Switzerland) with a thickness of 5 mm and placed into the measuring chamber. The low viscosity formulations were placed after stirring and removing the magnetic bar into a vacuum chamber and the vacuum was slowly reduced from 100 to 30 mbar during 20 min to eliminate air bubbles. Subsequently, the formulations were transferred to quartz cuvettes (thickness 5 mm for the aqueous and 10 mm for the 45% Transcutol in water formulation) and placed into the measuring chamber. Samples of the high viscosity formulations with tracer particles were manufactured as described above for the formulations except that no TOP-N53 was added and part of the water was replaced with the required amount of particle suspension at the beginning of the production process i.e., before adding the thickener. The final tracer particle concentration was 1% w/v for all high viscosity formulations apart from the high viscosity 45% Transcutol in water formulation with 2 200 nm tracer particles for which the concentration was 2% w/v. The formulations were stored for at least one week and were then transferred into a 10 mm quartz cuvette (with the exception of 5 mm for the aqueous formulation with 310 nm tracer particles) and allowed to rest at room temperature for 24 h before being placed into the measuring chamber.

The samples were equilibrated in the measuring chamber for 10 min (liquid and low viscosity formulations) or 20 min (high viscosity formulations) at 28°C. The l*-mode was set to auto and the refractive index to 1.329 and 1.383 for both liquid and low viscosity aqueous and 45% Transcutol in water formulations, respectively, and 1.339 and 1.387 for the high viscosity aqueous and 45% Transcutol

in water formulations, respectively. The measurement time was 360 s (including 60 s for the echo duration) for the liquid formulations and 1060 s including 60 s echo time for the low and the high viscosity formulations.

Three samples were prepared for every formulation and each sample was measured 3 to 5 times.

Data analysis

In the diffusion process of a particle in liquid media driven by Brownian motion the mean square displacement (MSD) is given by following equation:

$$MSD = 6(D0)\tau^{x} \qquad \text{Equation 1}$$

where D0 is the diffusion coefficient of the particle in the solvent, the exponent x accounts for possible sedimentation (x = 1 for no sedimentation) and τ is the lag time.

In presence of a thickener the movement of a particle is influenced by the polymer lattice. Three different regimes for the motion of the particles have been described [60]. At short time, the dynamic is still Brownian with the local diffusion coefficient D_0. At intermediate times, the MSD remains constant for a given time interval before the motion becomes diffusive again for longer times. The long-time diffusion coefficient Dm is influenced by the polymer lattice, thus corresponding to the macroscopic viscosity of the system. To describe these three regimes, the following equation was proposed:

$$MSD = 6\delta^2\left(1 - e^{-\left(\frac{D0}{\delta^2}\tau\right)^{\alpha}}\right)^{\frac{1}{\alpha}}\left(1 + \frac{Dm}{\delta^2}\tau\right) \qquad \text{Equation 2}$$

where δ^2 the amplitude of the motion of the particles and α accounts of the broad spectrum of relaxation times at the plateau onset time. The smaller the α the broader the relaxation spectrum.

Measured MSD data for the liquid formulations were fitted by Equation 1 and MSD data for low and high viscosity formulations by Equation 2 using the EASY-FIT® software [61]. From the least square regression analysis, values of the parameters were deduced.

2.4.5 HPLC-MS Assay

TOP-N53 its metabolite TOP-52 and their chemical degradation products were analyzed by a HPLC-UV-MS of Agilent series 1 200 equipped with a degaser G1379B, a binary pump G1312A, an autosampler G1367B, a thermostat G1330B, a column oven G1316A (series 1100), a variable wavelength detector G1314B, and a single quadrupole MS detector G6130A. A C-18 reversed phase column (Agilent ZORBAX Eclipse XDB-C18, 80 Å, 2.1 x 150 mm, 5 µm) and mobile phases (A) CH_3CN:H_2O (30:70) with 0.05% (v/v) formic acid and (B) CH_3CN:H_2O (90:10) with 0.05% (v/v) formic acid were used. The composition was varied in a gradient mode: 0 – 2 min 100:0 (A:B), 0 – 30 min linear change to 0:100 (A:B), 30 – 35 min 0:100 (A:B), 35 – 35.5 min linear change to 100:0 (A:B), and 35.5 – 45 min 100:0 (A:B) with a flow rate of 0.5 mL/min, and a runtime of 45 minutes. The samples were kept in the autosampler at 4°C, the injection volume was 30 µL and the column was heated to 60°C. The ions were generated by atmospheric pressure electrospray ionization and the MS detector was run in SIM mode at positive polarity with capillary voltage 4000 V, fragmentor 100 V, drying gas flow 10 L/min, drying gas temperature 350°C, and nebulizer pressure 20 psig. TOP-N53 was detected at 250 nm in UV and at m/z 605 in MS corresponding to the protonated form. The metabolite TOP-52 and the chemical degradation

products of TOP-N53 and TOP-52 were detected at 250 nm in UV and TOP-52 at m/z 560, *cis*-isomers of TOP-N53 and TOP-52 at m/z 605 and 560, respectively, and the aldehyde of TOP-N53 and TOP-52 at m/z 590 and 545, respectively, corresponding to their protonated forms. Chemical degradation products of TOP-N53 and TOP-52 were quantified with the calibration curve of TOP-N53 and TOP-52, respectively. The LOQ of TOP-N53 and TOP-52 were 0.01 µM in UV and 0.2 nM in MS. Linearity was fulfilled in UV for concentrations up to 100 µM and in MS 1 µM.

2.5 Statistical analysis

Results of the transport experiments for the donor compartment and the dermis obtained with the 100 µM TOP-N53 liquid, low and high viscosity aqueous and 45% Transcutol in water formulations were analyzed by two-way ANOVA using Excel (Microsoft, WA, USA).

3 RESULTS & DISCUSSION

3.1 *In vitro* wound model

Isolated pig skin dermis was employed to simulate the absence of epithelial barrier function in wound tissue. Drug treatment of chronic diabetic wounds is intended for wounds with Wagner grade 1 and less often zero and 2 [8]. In these instances, superficial ulcer with no exposure of tendon, bone or joint capsule is evident with compromised or complete absence of epidermis. Based on this, dermis represents an adequate tissue substrate to evaluate drug delivery in the open wound. The pharmacologic effect of TOP-N53 is exerted on the local vasculature enhancing blood flow, reducing endothelial dysfunction, and promoting angiogenesis [6, 7]. Use of dermis tissue which harbors extensive blood microcirculation, represented therefore also in this respect an appropriate *in vitro* model for the purpose of evaluating topical delivery of the used drug. To the best of the authors' knowledge there is only one previous study in which dermis was used as an *in vitro* wound drug delivery model to simulate ulcerated tissue [27].

The formulation was applied on the mounted dermis in the Franz diffusion cell typically with a thickness of 5 mm. This goes in hand with the depth of a superficial wound and the fact that in practice approximately a 5 mm layer of hydrogel is applied on the wound with a spatula [17]. The formulation was covered with the semi-permeable membrane Hydrofilm® to mimic the secondary dressing as in the clinic the wound and the hydrogel are covered with e.g. a gauze and closed also with a semi-permeable membrane [3, 17]. The latter is used to avoid occlusion which is not recommended for diabetic foot ulcers [3]. The *in vitro* transport experiment lasted three days (72 h) and the temperature was set to 28°C, these conditions simulating change of the dressing every 3rd day in a home care setting and the temperature of the foot ulcer [62-64]. This setting was used for all experiments apart from the ones with liquid aqueous formulations with the low and intermediate dose which served as introductory formulation screening.

Since dermis represents the target site of pharmacologic action, the amount of drug in this tissue was analyzed to assess transport kinetics. In addition, drug amount permeating in the basal compartment and remaining in the apical (donor) compartment were determined to reach a better understanding of local drug disposition and mass balance. Metabolic and chemical degradation drug products (Figure 1) were further assayed in all compartments. Major metabolite of TOP-N53 was TOP-52 which is formed through release of nitrogen oxide (NO) and is itself pharmacologically active. Photoisomerization yielding the *cis*-isomer was prevented as much as possible by working under exclusion of light while conversion to the aldehyde derivative was rather small. As an example, only 3.5% of chemical degradation products with respect to the applied drug amount (1.2% TOP-N53 *cis*-isomer, 1.2% TOP-52

cis-isomer, 0.4% TOP-N53 aldehyde and 0.7% TOP-52 aldehyde) was detected in the donor compartment 72 h after application of the 100 µM TOP-N53 aqueous liquid suspension formulation. Therefore, only the total amounts of TOP-N53 and its active metabolite TOP-52 comprising the sum of TOP-N53 and TOP-52 with their respective *cis*-isomer and aldehyde in each compartment are reported throughout this paper. Results reported for the donor compartment represent the sum of the amount found in the remainder of formulation, the glass wash and the wash of the tissue.

3.2 Microbial infection affecting TOP-N53 delivery

Experiments with and without addition of antibiotics and fungicide were performed in order to examine the role of microbial contamination in wounds on delivery of TOP-N53. Penicillin/streptomycin and amphotericin B were used as antibiotics and fungicide, respectively. An “off-line” bioconversion test with vehicle pre-exposed to dermis and skin transport experiments with the same drug formulation were performed. Figure 2a shows that TOP-N53 was metabolized to TOP-52 in the vehicle that was in contact with the dermis whereas no conversion happened in vehicle that had no previous contact with the tissue. The presence of antimicrobial agents in the medium that was pre-exposed to the dermis inhibited metabolism leading to the conclusion that microorganisms are likely responsible for the transformation of TOP-N53 to TOP-52 in the aqueous vehicle. This result also excludes the possibility that leaching of dermal enzymes into the vehicle was responsible for the bioconversion of the drug.

The same result was observed in the donor compartment in tissue transport experiment with 100 µM TOP-N53 liquid aqueous suspension formulation (Figure 2b). TOP-N53 amount decreased rapidly after 24 h and the amount of TOP-52 increased while in presence of the mixture penicillin/streptomycin/amphotericin B as well as of the antibiotic gentamicin sulfate no TOP-52 was formed in the donor compartment. Notably, the total amount of the compounds in the donor compartment is constant over time with and without antimicrobial compounds.
TOP-N53 delivery into the dermis increased continuously with time but only a small amount (approx. 0.5 nmol) of TOP-N53 was delivered during 72 h regardless of the presence of antibiotics and fungicide and regardless of the decrease of TOP-N53 in the donor over time when no antimicrobial agents were present. Delivery of TOP-N53 using different formulation approaches is discussed below. Interestingly, more TOP-52 than TOP-N53 was delivered into the dermis when no antimicrobial agents were used. This increase parallels the increased amount of TOP-52 in the donor compartment and suggests that no TOP-52 was formed in the dermis. This notion was confirmed in the two experiments containing antimicrobial agents in which no TOP-52 was found in the dermis. The comparative propensity of TOP-N53 and TOP-52 to penetrate into dermis is evaluated in the following section. No TOP-N53 and only a small permeation of TOP-52 was found in the acceptor compartment at 72 h.

Hence, microbial contamination of drug preparations may lead to bioconversion of the active ingredient and penetration of metabolite into the tissue leading to an overall increase of delivery which may be beneficial in case the metabolite also exhibits pharmacologic activity. This observation is relevant for clinical praxis since chronic wounds may frequently be subject to opportunistic infection despite regular care.

3.3 Effect of liquid formulation type

To modulate and increase TOP-N53 delivery, liquid formulations using on one hand (purely) aqueous vehicle based on PBS and on the other hand a 45% Transcutol in water vehicle were developed. In the aqueous formulations, the drug substance was either solubilized by encapsulation in colloidal particles consisting of surfactant micelles or phospholipid liposomes or was present in the form of suspended micro-particles. TOP-N53 has a high lipophilicity (milogP 6.2) and is completely insoluble with no

measurable solubility in purely aqueous media. The API was stably solubilized at a concentration of 10 µM suggesting complete entrapment in the colloidal particles. Stirred media milling used to prepare micro-particles seemed to affect API crystallinity as determined by solid phase analysis (Fig, S1, Fig. S2, Fig. S3, supplementary information). Even though this may transiently affect solubility, dermal delivery results of the suspension formulations are considered to be determined by the equilibrium solubility of the compound (for additional discussion see supplementary information). Notably, the solubility of TOP-N53 in 45% Transcutol in water vehicle is around 20 µM. Therefore, in the latter formulations with a drug content below 20 µM the compound was fully dissolved while for higher drug content the compound was partly dissolved and partly suspended. The characteristics of the formulations can be taken from Table 1.

Figure 3 shows the effect of the liquid formulations and applied amounts and concentrations of TOP-N53 on the delivery of the drug into the dermis at the time point of 48 h. No antimicrobial agents were involved in these transport experiments.

For aqueous formulations with the lowest TN53 dose (7.5 and 3.4 nmol) only a small TOP-N53 amount of 0.049 and 0.036 nmol was delivered to the dermis with the micellar and suspension formulation, respectively. With an increase of the dose to 40 and 33 nmol for the micellar and suspension formulation, respectively by increasing the applied volume while keeping the drug concentration/content at roughly the same level, more TOP-N53 (0.11 nmol) was delivered in the dermis with the suspension formulation but not with the micellar formulation. This was not surprising for the micellar formulation as the concentration of solubilized drug, which remained the same, is the driving force for mass transport. For the aqueous suspension formulation, in which no drug is dissolved, the increased dermis delivery of TOP-N53 observed at the higher dose is attributed to sedimentation of particles leading to a higher drug mass on the dermis surface. This interpretation was supported by a further increase of the dose of the aqueous suspension from 40 to 100 nmol by increasing the TOP-N53 content in the formulation from 10 to 100 µM. This highest dose (100 nmol) further increased the amount delivered to the dermis from 0.11 to 0.27 nmol. It appears, therefore, that the suspension formulation provides a dose-dependent delivery presumably due to settling of drug particles onto the tissue. The liposomal formulation provided at a comparable dose similarly low delivery as the micellar formulation. Drug solubilization in liposomes, therefore, had a similar effect on delivery as solubilization in micelles, the somewhat higher amount found in the tissue with the former being possibly attributable to sedimentation of liposomes on the tissue surface. It is noted that concentration of solubilized drug could not be further increased in the micellar formulation due to limited solubility of TOP-N53 at the used surfactant concentration (solubility = 13 µM).

For all aqueous TOP-N53 formulations, more TOP-52 was delivered into the dermis than TOP-N53 regardless of the dose applied and the content of TOP-N53 in the formulation (Figure 3). As shown above, TOP-52 is formed in the donor compartment containing the formulation by microbial enzymes and then diffuses into the tissue. Nevertheless, the proportion of TOP-52 to TOP-N53 found in the dermis did not reflect their proportion in the donor compartment for the different doses and drug content applied. For the suspension formulations, this would suggest that the aqueous solubility of TOP-52 is higher than that of TOP-N53. The transport experiment with the micellar formulation containing TOP-52 revealed that this compound might have a higher propensity to penetrate into dermis from this formulation compared to TOP-N53.

Finally, only a small amount of TOP-52 was found in the acceptor compartment varying between 0.018 nmol for the liposomal formulation, 0.088 nmol and 0.094 nmol for the micellar formulation with low and intermediate dose, respectively, and 0.059 nmol and 0.19 nmol for the suspension formulation with low and intermediate dose, respectively. No TOP-52 was detected for the high dose suspension formulation and 0.035 nmol was found for the micellar formulation with TOP-52. No TOP-N53 was detected in the acceptor compartment with any of the formulations.

Considerably more TOP-N53 was delivered into the dermis with the 10 µM Transcutol in water formulation compared to the low dose (>20 fold) and even high dose (3.7-fold) aqueous suspension formulations. This demonstrates that presence of TOP-N53 in molecularly dissolved form in this formulation enhances diffusion of the compound into the tissue compared, for instance, to the aqueous suspension formulation. The results also show that dissolution of TOP-N53 is much more efficient in terms of delivery compared to its solubilization in micelles or liposomes probably because the compound must be released from these colloidal structures before it can diffuse into the tissue. A second possible explanation of the high drug delivery obtained with this formulation is the well-known property of Transcutol to partition into the dermis thereby reducing water activity and increasing solubility of the drug in the dermis [38]. Increase of TOP-N53 content from 10 to 100 µM in Transcutol/water yielded a suspension formulation containing partly dissolved drug which delivered slightly more (1.5-fold) drug into the dermis than the solution formulation. This correlated roughly with the twice higher dissolved concentration of TOP-N53 in this formulation (solubility of TOP-N53 in 45% Transcutol in water = 20 µM) compared to the 10 µM solution. The sedimentation process discussed above for the aqueous suspension formulations seems therefore to play a minor role in this case. Only a small amount of TOP-52 was found in the dermis, regardless of the dose applied, which was less than TOP-N53 contrary to the results of the aqueous formulation and goes hand in hand with the low amount of TOP-52 found in the donor compartment.

These findings suggest that bioconversion of TOP-N53 in the donor compartment was inhibited by Transcutol. Bioconversion test results (Figure 4a) confirmed that no TOP-52 was formed in the presence of Transcutol. As many organic solvents, Transcutol reduces water activity that is expected to be 0.91 for 45% Transcutol in water (extrapolated from Björklund et al. [65]). Proliferation of water born microorganisms requires a minimum water activity of 0.95. Skin microorganisms such as staphylococci and micrococci reportedly tolerate a lower water activity of a minimum of 0.87. Therefore, the water activity of around 0.91 may be expected to reduce bacterial growth and therefore drug bioconversion in these formulations [66].

Although more TOP-N53 was found in the dermis for the Transcutol in water formulations no TOP-N53 and no TOP-52 were found in the acceptor with the solution formulation and only 0.030 nmol TOP-52 was detected with the suspension formulation. Transcutol is expected to substantially increase osmolality of the formulations even though an exact osmolality value for the 45% Transcutol in water vehicle could not be determined due to lack of crystallization in the measurement (see Table 2). In fact, a bulging of the Hydrofilm® membrane covering the donor compartment of the diffusion cells was observed when the regularly employed isotonic 1% Kolliphor ELP in PBS was present in the acceptor. This was probably due to water flux from the acceptor into the donor compartment caused by the big difference of osmotic pressure between the two solutions. To investigate the influence of this osmolality difference and of the composition of the acceptor solution, in general, on measured drug delivery to the tissue, transport experiments were also conducted with the 100 µM TOP-N53 45% Transcutol in water formulation with a 45% Transcutol in water solution added to the acceptor compartment instead of 1% Kolliphor ELP in PBS. A relatively large amount of TOP-N53 permeated in the acceptor compartment in this experiment (Figure 4b). In fact, this was the only case in which TOP-N53 was detected in the acceptor solution. Moreover, less TOP-N53 was found in the dermis in this experiment compared to when 1% Kolliphor ELP in PBS was used as acceptor solution. These results indicate that accumulation of TOP-N53 in the dermis may occur due to high affinity of the drug for the tissue compared to the acceptor solution. In addition, osmotic water flux may impede drug diffusion through the dermis and entry into the acceptor compartment. Hence, besides enhancing solubility and inhibiting metabolism, Transcutol exerts an osmotic effect on drug delivery. A schematic representation of the delivery process of TOP-N53 into the dermis after applying liquid formulations is shown in Figure 5.

Taken together, rather low tissue delivery of TOP-N53 is achieved with the used aqueous formulations as a result of its poor water solubility and high lipophilicity which hinder drug diffusion and penetration into the hydrophilic dermis. Since lipophilic formulations causing occlusion are avoided in clinical

practice of treatment in order to reduce the risk of bacteria proliferation in the wound, water-based vehicles should be used. Colloidal solubilization of the drug substance is shown not to enhance delivery to any notable extent while the positive effect of suspension formulation that is attributed to sedimentation is not practically relevant for the treatment of diabatic wounds in the lower extremities (foot soles etc.). Dissolution of the drug substance in a formulation containing a water-miscible cosolvent provided the highest delivery and seems, therefore, to be the most promising approach. A constant delivery for a few days was measured in the latter case as shown in Figure 4b and discussed in the following section of this article and the delivery rate appears to be such that, with the applied formulation amount tailored to match the depth of the wound, a drug supply for approximately half a week could be guaranteed. This would be in line with the frequency of change of wound dressings during regular home care. The locally delivered drug amount can be estimated to be sufficient for a pharmacologic effect of TOP-N53. Ben-Yehuda et al. observed an effect in *in vivo* animal studies already after injecting 0.2 nmol TOP-N53 intradermally at the wound edge [7].

3.4 Effect of formulation viscosity

Application of a liquid formulation on a diabetic foot ulcer on a regular basis, nevertheless, may not be appropriate from a practical perspective. The possibility to maintain disposition of a sufficient amount of drug product to lower extremities, dilution by wound secretions and/or absorption into wound dressings represent notable problems. For this reason, viscous hydrogel formulations were developed on the basis of the studied liquid ones. A low viscosity formulation with moisturizing potential for dry wounds and a high viscosity formulation for wet wounds with the capacity to take up superfluous liquid were investigated. The viscosity of the developed gel formulations was matched with that of commercial wound care products (e.g., Hydrosorb® Gel from Paul Hartmann AG and Intrasite Gel from Smith & Nephew AG). One hundred µM TOP-N53 aqueous and 45% Transcutol in water suspension formulations with low and high viscosity were developed. Both types of liquid formulation vehicle were used for the sake of comparison and their characteristics can be taken from Table 2.

The effect of viscosity on the amount versus time profiles of the *in vitro* transport experiments is shown in Figure 6. No TOP-N53 was delivered to the dermis with the aqueous high viscosity gel formulation whereas no difference is obvious over the entire time scale between low viscosity and liquid aqueous formulations. In the donor compartment, TOP-N53 content of the aqueous liquid formulation decreased as a function of time whereas this decrease was abated for the high viscosity formulation. In agreement with this result, the amount of TOP-52 formed by bioconversion of TOP-N53 in the donor compartment (see discussion above) was smaller for the high viscosity than for the other formulations. The amount of TOP-52 delivered to the dermis, however, did not differ between the three aqueous formulations. For the 45% Transcutol in water formulations, a steady increase of the delivered TOP-N53 amount into the dermis as a function of time is evident over 72 hours. This delivery however, decreased with increasing viscosity. Bioconversion in the donor compartment was inhibited (as discussed above) for all three formulations.

The reduction of TOP-N53 delivery in the dermis at increased formulation viscosity was highly significant as determined by two-way ANOVA (Table 3). The presence of Transcutol was responsible for a highly significant increase of dermis delivery of TOP-N53 (Table 3) which can be explained by the higher solubility of the drug in this vehicle as discussed above. The effect of viscosity in reducing drug delivery to the dermis applies to both, the aqueous and the Transcutol in water formulations. The magnitude of this effect might be different between the two formulation types as the significant ($p < 0.05$) interaction (Table 3) would suggest, this result, however, must be taken with precaution as the effect is 4.5-fold between low viscosity and liquid formulation for both with and without Transcutol. It remains nevertheless very interesting that delivery is impeded by increased viscosity regardless of the presence of dissolved drug compound in the formulation. This aspect is discussed in more detail in the following

section. Contrary to TOP-N53, the delivery of TOP-52 was significantly affected only by the presence of Transcutol but not by viscosity. This is because Transcutol inhibited TOP-52 formation as confirmed by the results of the donor compartment.

Bioconversion of TOP-N53 to TOP-52 in the donor compartment was reduced with high significance by the increase of viscosity and the presence of Transcutol (Table 4). The effect of viscosity was more pronounced in the purely aqueous formulation as nearly no bioconversion occurred in presence of Transcutol giving rise to a significant interaction (Table 4). This effect of viscosity on bioconversion is rather unexpected and might be related to a reduced mobility of drug particles and possibly microorganisms in the viscous formulation (for a graphical representation see Figure 5). Viscosity, however, did not influence TOP-52 delivery into the dermis.

Sedimentation of drug micro-particles on tissue surface was implicated above for the interpretation of delivery results to the dermis of suspension formulations. To test this hypothesis, the drug amount recovered from the dermis surface by the dermis wash was evaluated for the aqueous and the Transcutol in water formulations with different viscosities. The results in (Figure 7) demonstrate that settling of drug on the tissue surface was reduced by the increasing formulation viscosity for both types of formulation. Hence, the retarding effect of viscosity on TOP-N53 delivery appears to be related to reduced sedimentation of the particles within the gel formulation. Interestingly, however, the effect of viscosity is also evident for the Transcutol in water formulations, in which, in addition to the micro-particles, a marked proportion of drug exists in a molecularly dissolved form.

3.5 Rheological and diffusion analysis

To better understand the role of formulation viscosity for drug delivery and examine a possible correlation between the obtained results of the transport experiments and the rheological properties of the used formulations, macro- and micro-rheological properties and diffusive behavior of particles in the gel formulations were studied using on one hand diffusive wave spectroscopy (DWS) with two different sizes of tracer particles (310 and 2 200 nm) and on the other hand mechanical rheology (oscillation test).

Mean square displacement (MSD) as a function of lag-time obtained from DWS measurements characterizing the diffusional movement of particles within the formulation is shown for the liquid, low viscosity and high viscosity gel formulation in Figure 8. By fitting Eq. 1 and Eq. 2 to the data of liquid and gel formulations, respectively, the local diffusion coefficient (D_0), the long-time diffusion coefficient (Dm), the amplitude of the motion of the particles (δ^2) and the exponents x and α were deduced (Table 5).
The mean square displacement data for small (310 nm) and large (2 200 nm) tracer particles in the liquid aqueous and Transcutol in water formulation was almost linear (x: between 1 and 1.15). The deduced local diffusion coefficient (D_0) from Eq. 1 was highest for the small particles in liquid aqueous formulation (2'179'805 nm^2/s), while a 3-fold smaller D_0 was obtained for the large particles. For the Transcutol in water liquid formulation, approximately 5- and 4-fold smaller D_0 values compared to the respective values of the aqueous formulation for the small and the large particles, respectively, were obtained which is consistent with the roughly 3-fold difference in viscosity between the two formulations (Table 1).

In the gel formulations, the local diffusion coefficient of particles within the cage of the polymer lattice was assumed to be the same as in liquid [60] and was therefore, kept constant at the value obtained from Eq. 1 (liquid formulations) when fitting Eq. 2 to the MSD data of both gel formulations. Deduced Dm values were a lot smaller than D_0 values denoting the restriction imposed by the polymer lattice on the diffusion of particles (Table 5). Dm values nevertheless were higher for the low viscosity gel formulation than for the high viscosity one for both aqueous and Transcutol in water formulations

whereas Dm values of the aqueous formulations were higher than the respective values of the Transcutol in water formulations. The resulting long-time diffusion coefficient (Dm) shows how diffusion of particles is influenced by the polymer lattice and is therefore a reflection of the macroscopic viscosity of the gel. Small tracer particles exhibited higher Dm values than large tracer particles in both high viscosity gel formulation while the opposite was true for the low viscosity gel formulations. The latter was surprising and was probably due to some aggregation observed for the small tracer particles possibly as a result of interaction with the sodium carboxymethylcellulose used as thickener. No such aggregation was observed for the large tracer particles.

Deduced values of the amplitude of the motion of the particles (δ^2), also referred to as apparent cage size [54, 60], were congruent with the long-time diffusion coefficient Dm, for all gel formulations and both tracer particle sizes (Table 5). Finally, deduced values of the exponent α which accounts for the spectrum of relaxation time at the plateau onset [60], were comparable for all gel formulations and low (around 0.1) indicating a wide relaxation spectrum.

These results demonstrate a strong restriction of diffusion of particles by the polymer lattice of the gel formulations which correlated with the deduced apparent cage size and was accentuated by the high viscosity gel formulation as compared to the low viscosity gel formulation and by the presence of Transcutol in the vehicle. Considerable differences with respect to rheological properties between gel formulations of different composition are hence evident.

A further insight into the properties of the used gel formulations is attained by viscoelasticity analysis (Figure 9). Micro-rheological measurements by DWS and macro-rheological measurements by mechanical oscillation test yielded higher viscous (loss) moduli (G'') than elastic (storage) moduli (G') for the low viscosity gel formulation over a wide range of frequencies, the elastic modulus approaching the viscous modulus at high frequencies. Hence, the low viscosity gel formulation exhibited a liquid-like behavior. This was true for the aqueous as well as the Transcutol in water formulations. Interestingly, the moduli obtained by mechanical oscillation test coincide with those obtained by DWS measurement with the large tracer particles. This indicates that DWS measurements of this formulation with the 2 200 nm tracer particles reflect exactly the macroscopic properties of the gel structure. For the high viscosity gel formulation, elastic modulus (G') was higher than viscous modulus (G'') indicating that these formulations possessed solid-like characteristics (Table 2 and Figure 9).

The liquid-like behavior of the low viscosity gel formulations is indicative of a flexible structure of the polymer lattice of the gel and concurs with the considerably higher estimated long-time diffusion coefficient, Dm, compared to that of the high viscosity gel formulation. The solid-like behavior exhibited by the latter is consistent with a rigid polymer lattice of the gel ever strongly limiting diffusion.

3.6 Formulation rheology affecting drug delivery

Based on these results, the distance of diffusion of a particle with a size of 2 200 nm in the aqueous formulations, for example, may be estimated using Eq. 1 and Eq. 2. In a time interval of 3 days corresponding to a typical duration of application of a drug product to a chronic diabetic wound, this distance is 2.6 mm for the aqueous liquid formulation, 0.052 mm for the low viscosity aqueous gel formulation and only 513 nm for the high viscosity aqueous gel formulation. Considering that the layer thickness of formulation applied was 5 mm and even though these distances are statistical estimates, it is not surprising that less TOP-N53 was delivered into the dermis with the low viscosity compared to the liquid formulation and no drug was delivered with the high viscosity formulation. Sedimentation of undissolved drug particles onto the tissue surface was implicated in the above discussion as a mechanism promoting delivery to the tissue. The present rheological analysis provides of course information about the diffusional behavior of particles. It can be reasonably argued, however, that the

restriction imposed by the polymer lattice of the gel to diffusion will also apply, at least in qualitative terms, to particle movement by sedimentation. Hence, rheological properties of formulation are shown to correlate with their drug delivery performance in the *in vitro* transport studies.

The statistical analysis carried out showed that gel formulations elicited a reduction of drug delivery also in the Transcutol in water formulations, in which drug is contained to a large part in dissolved form. It is not possible using DWS data to reliably predict whether the polymer lattice of the gel restricts diffusion of drug molecules. An extrapolation of the data of small and large tracer particles to molecular size of 1 nm by the Stokes-Einstein relation provides a diffusion coefficient in the liquid Transcutol in water formulation of the order of magnitude expected for fluids (8.92×10^{-7} cm^2/s) while a 10^6 times smaller value is obtained for the high viscosity Transcutol in water gel formulation, this value still being much higher than the Dm values of the tracer particles. Granted that this argument is ambiguous, one can still not rule out the possibility that restricted diffusion of drug molecules by the polymer lattice is in part responsible for the diminished drug delivery observed with these gel formulations compared to the liquid one. Alternatively, or possibly in addition, specific molecular interaction of drug molecules with polymer chains of the gel may account for the reduction of drug delivery [45, 67, 68]. NMR dosy measurements may help resolve this question.

Statistical analysis, furthermore, suggested that bacterial metabolism of TOP-N53 in the aqueous formulations was hindered by increased formulation viscosity (Table 4). Considering that bacteria have a size of around 1 µm it can be suggested that their movement within the formulation may be restricted by the polymer lattice of the gel just as the diffusion of drug particles. This would reduce the probability that bacteria and drug particles get in contact with each other resulting in less metabolite formed. Rheology of formulation, therefore, seems not only to influence drug delivery to the tissue but also drug bioconversion. However, reduced formation of TOP-52 in the donor compartment was not reflected in the delivery of TOP-52 into the dermis (Table 3). Conceivably, this was because bioconversion took place mostly at the surface of the dermis as diffusion in the gel formulations was restricted, giving the metabolite immediate access into the tissue (Figure 5). Therefore, no differences could be observed in the dermis.

4 CONCLUSION

Water-miscible cosolvent (Transcutol) improving solubility in a water-based vehicle is crucial for significantly enhancing delivery of the poorly water-soluble and highly lipophilic API TOP-N53 into the dermis and was shown to be the only formulation approach that provided sufficient drug amount in the tissue for eliciting pharmacologic effect. Sustained drug delivery over a three-day period could be achieved. In addition, Transcutol suppressed opportunistic infection and inhibited microbial metabolism of the drug. The latter can be responsible for considerable degradation of the active ingredient applied to the tissue. It should be kept in mind, however, that the cosolvent approach can cause osmotic water flow out of the tissue. Hydrogels with increased viscosity representing clinically relevant drug formulations may result in a significant reduction of the delivered drug amount in a viscosity dependent fashion. Micro-rheologic analysis of hydrogels confirms the restricted movement of drug microparticles and possibly molecules in the gel which can be responsible for reduced drug delivery. The practical advantage of high viscosity formulations of being more user friendly and having good applicatory characteristics must, therefore, counterbalance their adverse impact on drug delivery. The present work integrates *in vitro* wound model development for drug delivery assessment and formulation of a new API with primary and secondary dressing considerations and provides mechanistic insights and an implementation concept for the treatment of chronic diabetic foot ulcer under home care conditions.

5 ACKNOWLEDGEMENT

This project was financially supported by Innosuisse project number 25840.1 PFLS-LS in collaboration with Topadur Pharma AG. The authors thank PD Dr. med. Martin Berli of the Balgrist University Hospital, Zurich and Barbara Seitzinger-Mäder of the Wund-Praxis Seitzinger GmbH, Basel for valuable insights into the clinical practice of chronic diabetic wound treatment.

6 REFERENCES

[1] IDF. "IDF Diabetes Atlas." IDF. https://diabetesatlas.org/idfawp/resource-files/2021/07/IDF_Atlas_10th_Edition_2021.pdf (accessed 25th May 2022).

[2] D. Baltzis, I. Eleftheriadou, and A. Veves, "Pathogenesis and treatment of impaired wound healing in diabetes mellitus: New insights," *Adv Ther,* vol. 31, no. 8, pp. 817-36, 2014, doi: 10.1007/s12325-014-0140-x.

[3] A. Veves, J. M. Giurini, and R. J. Guzman, Eds. *The Diabetic Foot*, 4th ed. Cham, Switzerland: Springer Nature Switzerland AG, 2018.

[4] WHO. "Global report on diabetes." WHO Press. https://apps.who.int/iris/bitstream/handle/10665/204871/9789241565257_eng.pdf (accessed 25th May 2022).

[5] C. K. Sen, "Human wounds and its burden: An updated compendium of estimates," *Adv Wound Care (New Rochelle),* vol. 8, no. 2, pp. 39-48, 2019, doi: 10.1089/wound.2019.0946.

[6] R. Naef, H. Tenor, and G. Koch, "TOP-N53: A clinical drug candidate for the treatment of non-healing wounds," *Chimia (Aarau),* vol. 74, no. 10, pp. 814-817, 2020, doi: 10.2533/chimia.2020.814.

[7] M. Ben-Yehuda Greenwald *et al.*, "A dual-acting nitric oxide donor and phosphodiesterase 5 inhibitor promotes wound healing in normal mice and mice with diabetes," *J Invest Dermatol,* vol. 141, no. 2, pp. 415-426, 2021, doi: 10.1016/j.jid.2020.05.111.

[8] F. W. Wagner, "The dysvascular foot: A system for diagnosis and treatment," *Foot Ankle,* vol. 2, no. 2, pp. 64-122, 1981, doi: 10.1177/107110078100200202.

[9] J. Sowada, A. Schmalenberger, I. Ebner, A. Luch, and T. Tralau, "Degradation of benzo[a]pyrene by bacterial isolates from human skin," *FEMS Microbiol Ecol,* vol. 88, no. 1, pp. 129-39, 2014, doi: 10.1111/1574-6941.12276.

[10] J. Sun, J. Jin, R. D. Beger, C. E. Cerniglia, and H. Chen, "Evaluation of metabolism of azo dyes and their effects on Staphylococcus aureus metabolome," *J Ind Microbiol Biotechnol,* vol. 44, no. 10, pp. 1471-1481, 2017, doi: 10.1007/s10295-017-1970-8.

[11] S. K. Jaiswal, S. M. Agarwal, P. Thodum, and V. K. Sharma, "SkinBug: An artificial intelligence approach to predict human skin microbiome-mediated metabolism of biotics and xenobiotics," *iScience,* vol. 24, no. 1, p. 101925, 2021, doi: 10.1016/j.isci.2020.101925.

[12] L. Wu, G. Norman, J. C. Dumville, S. O'Meara, and S. E. Bell-Syer, "Dressings for treating foot ulcers in people with diabetes: An overview of systematic reviews," *Cochrane Database Syst Rev,* no. 7, p. CD010471, 2015, doi: 10.1002/14651858.CD010471.pub2.

[13] J. C. Dumville, S. O'Meara, S. Deshpande, and K. Speak, "Alginate dressings for healing diabetic foot ulcers," *Cochrane Database Syst Rev,* no. 6, p. CD009110, 2013, doi: 10.1002/14651858.CD009110.pub3.

[14] J. C. Dumville, S. Deshpande, S. O'Meara, and K. Speak, "Foam dressings for healing diabetic foot ulcers," *Cochrane Database Syst Rev,* no. 6, p. CD009111, 2013, doi: 10.1002/14651858.CD009111.pub3.

[15] J. C. Dumville, S. Deshpande, S. O'Meara, and K. Speak, "Hydrocolloid dressings for healing diabetic foot ulcers," *Cochrane Database Syst Rev,* no. 8, p. CD009099, 2013, doi: 10.1002/14651858.CD009099.pub3.

[16] J. C. Dumville, S. O'Meara, S. Deshpande, and K. Speak, "Hydrogel dressings for healing diabetic foot ulcers," *Cochrane Database Syst Rev,* no. 7, p. CD009101, 2013, doi: 10.1002/14651858.CD009101.pub3.

[17] A. Vasel-Biergans and W. Probst, *Wundauflagen für die Kitteltasche*, 3rd ed. Stuttgart, Germany: Wissenschaftliche Verlagsgesellschaft Stuttgart, 2010.

[18] H. Wu *et al.*, "The promising hydrogel candidates for preclinically treating diabetic foot ulcer: A systematic review and meta-analysis," *Adv Wound Care (New Rochelle),* 2022, doi: 10.1089/wound.2021.0162.

[19] Smith&Nephew. "REGRANEX ◊ (becaplermin) Gel, 0.01%." Smith&Nephew Inc. https://www.smith-nephew.com/key-products/advanced-wound-management/regranex-becaplermin-gel/ (accessed 15th May 2022).

[20] V. V. Karri, G. Kuppusamy, S. V. Talluri, K. Yamjala, S. S. Mannemala, and R. Malayandi, "Current and emerging therapies in the management of diabetic foot ulcers," *Curr Med Res Opin,* vol. 32, no. 3, pp. 519-42, 2016, doi: 10.1185/03007995.2015.1128888.

[21] P. P. Shah, P. R. Desai, A. R. Patel, and M. S. Singh, "Skin permeating nanogel for the cutaneous co-delivery of two anti-inflammatory drugs," *Biomaterials,* vol. 33, no. 5, pp. 1607-17, 2012, doi: 10.1016/j.biomaterials.2011.11.011.

[22] OECD. Test No. 428: Skin Absorption: In Vitro Method," 2004, doi: https://doi.org/10.1787/9789264071087-en.

[23] OECD, "*Guidance Document for the Conduct of Skin Absorption Studies* , OECD Series on Testing and Assessment, No. 28," 2004, doi: https://doi.org/10.1787/9789264078796-en.

[24] V. P. Shah, J. Jenner, and H. I. Maibach, Eds. *Topical Drug Bioavailability, Bioequivalence, and Penetration*, 2nd ed. New York, NY, USA: Springer, 2014.

[25] U. Jacobi *et al.*, "Porcine ear skin: An in vitro model for human skin,"*Skin Res Technol,* vol. 13, no. 1, pp. 19-24, 2007, doi: 10.1111/j.1600-0846.2006.00179.x.

[26] F. C. Arnold, G. Hutchinson, JJ. Weston-Davies, W., "The Wound Healing Society, the European Tissue Repair Society and the Japanese Society for Wound Healing," *Wound Rep Regen,* vol. 4, no. 1, pp. 121-126, 1996, https://doi.org/10.1046/j.1524-475X.1996.40119.x.

[27] M. Walker *et al.*, "In vitro model(s) for the percutaneous delivery of active tissue repair agents," *J Pharm Sci,* vol. 86, no. 12, pp. 1379-84, 1997, doi: 10.1021/js970159i.

[28] H. Dabboue, N. Builles, E. Frouin, D. Scott, J. Ramos, and G. Marti-Mestres, "Assessing the impact of mechanical damage on full-thickness porcine and human skin using an in vitro approach," *Biomed Res Int,* vol. 2015, p. 434623, 2015, doi: 10.1155/2015/434623.

[29] S. Dey *et al.*, "An in vitro skin penetration model for compromised skin: Estimating penetration of polyethylene glycol [^{14}C]-PEG-7 phosphate," *Skin Pharmacol Physiol,* vol. 28, no. 1, pp. 12-21, 2015, doi: 10.1159/000362284.

[30] S. Pažoureková, J. Hojerová, Z. Klimová, and M. Lucová, "Dermal absorption and hydrolysis of methylparaben in different vehicles through intact and damaged skin: Using a pig-ear model in vitro," *Food Chem Toxicol,* vol. 59, pp. 754-65, 2013, doi: 10.1016/j.fct.2013.07.025.

[31] D. J. Davies, J. R. Heylings, T. J. McCarthy, and C. M. Correa, "Development of an in vitro model for studying the penetration of chemicals through compromised skin," *Toxicol In Vitro,* vol. 29, no. 1, pp. 176-81, 2015, doi: 10.1016/j.tiv.2014.09.012.

[32] D. J. Davies, J. R. Heylings, H. Gayes, T. J. McCarthy, and M. C. Mack, "Further development of an in vitro model for studying the penetration of chemicals through compromised skin," *Toxicol In Vitro,* vol. 38, pp. 101-107, 2017, doi: 10.1016/j.tiv.2016.10.004.

[33] P. Dong *et al.*, "Barrier-disrupted skin: Quantitative analysis of tape and cyanoacrylate stripping efficiency by multiphoton tomography," *Int J Pharm,* vol. 574, p. 118843, 2020, doi: 10.1016/j.ijpharm.2019.118843.

[34] K. Ganesh, M. Sinha, S. S. Mathew-Steiner, A. Das, S. Roy, and C. K. Sen, "Chronic wound biofilm model," *Adv Wound Care (New Rochelle),* vol. 4, no. 7, pp. 382-388, 2015, doi: 10.1089/wound.2014.0587.

[35] F. Zhou, Z. Song, Y. Wen, H. Xu, L. Zhu, and R. Feng, "Transdermal delivery of curcumin-loaded supramolecular hydrogels for dermatitis treatment," *J Mater Sci Mater Med,* vol. 30, no. 1, p. 11, 2019, doi: 10.1007/s10856-018-6215-5.

[36] A. Hussain, M. A. Altamimi, S. Alshehri, S. S. Imam, and S. K. Singh, "Vesicular elastic liposomes for transdermal delivery of rifampicin: In-vitro, in-vivo and in silico GastroPlus™ prediction studies," *Eur J Pharm Sci,* vol. 151, p. 105411, 2020, doi: 10.1016/j.ejps.2020.105411.

[37] A. Bhatia, R. Kumar, and O. P. Katare, "Tamoxifen in topical liposomes: Development, characterization and in-vitro evaluation," *J Pharm Pharm Sci,* vol. 7, no. 2, pp. 252-9, 2004.

[38] D. W. Osborne and J. Musakhanian, "Skin penetration and permeation properties of Transcutol®-neat or diluted mixtures," *AAPS PharmSciTech,* vol. 19, no. 8, pp. 3512-3533, 2018, doi: 10.1208/s12249-018-1196-8.

[39] FDA. "Inactive ingredient search for approved drug products." FDA. https://www.accessdata.fda.gov/scripts/cder/iig/index.cfm (accessed 17th August 2020).

[40] C. Tas, Y. Ozkan, A. Savaser, and T. Baykara, "In vitro release studies of chlorpheniramine maleate from gels prepared by different cellulose derivatives," *Farmaco,* vol. 58, no. 8, pp. 605-11, 2003, doi: 10.1016/S0014-827X(03)00080-6.

[41] N. Kanpipit, N. Nualkaew, W. Kiatponglarp, A. Priprem, and S. Thapphasaraphong, "Development of a sericin hydrogel to deliver anthocyanins from purple waxy corn cob (Zea mays L.) extract and in vitro evaluation of anti-inflammatory effects," *Pharmaceutics,* vol. 14, no. 3, 2022, doi: 10.3390/pharmaceutics14030577.

[42] N. Dragicevic-Curic *et al.*, "Temoporfin-loaded liposomal gels: Viscoelastic properties and in vitro skin penetration," *Int J Pharm,* vol. 373, no. 1-2, pp. 77-84, 2009, doi: 10.1016/j.ijpharm.2009.02.010.

[43] R. A-sasutjarit, A. Sirivat, and P. Vayumhasuwan, "Viscoelastic properties of Carbopol 940 gels and their relationships to piroxicam diffusion coefficients in gel bases," *Pharm Res,* vol. 22, no. 12, pp. 2134-40, 2005, doi: 10.1007/s11095-005-8244-2.

[44] L. Binder, J. Mazál, R. Petz, V. Klang, and C. Valenta, "The role of viscosity on skin penetration from cellulose ether-based hydrogels," *Skin Res Technol,* vol. 25, no. 5, pp. 725-734, 2019, doi: 10.1111/srt.12709.

[45] J. A. Ji *et al.*, "Characteristics of rhVEGF release from topical hydrogel formulations," *Pharm Res,* vol. 27, no. 4, pp. 644-54, 2010, doi: 10.1007/s11095-009-0039-4.

[46] K. I. Al-Khamis, S. S. Davis, and J. Hadgraft, "Microviscosity and drug release from topical gel formulations," *Pharm Res,* vol. 3, no. 4, pp. 214-7, 1986, doi: 10.1023/A:1016386613239.

[47] T. Pongjanyakul and S. Puttipipatkhachorn, "Sodium alginate-magnesium aluminum silicate composite gels: Characterization of flow behavior, microviscosity, and drug diffusivity," *AAPS PharmSciTech,* vol. 8, no. 3, p. E72, 2007, doi: 10.1208/pt0803072.

[48] J. Hurler and N. Skalko-Basnet, "Potentials of chitosan-based delivery systems in wound therapy: Bioadhesion study," *J Funct Biomater,* vol. 3, no. 1, pp. 37-48, 2012, doi: 10.3390/jfb3010037.

[49] C. Alvarez-Lorenzo, J. L. Gómez-Amoza, R. Martínez-Pacheco, C. Souto, and A. Concheiro, "Microviscosity of hydroxypropylcellulose gels as a basis for prediction of drug diffusion rates," *Int J Pharm,* vol. 180, no. 1, pp. 91-103, 1999, doi: 10.1016/s0378-5173(98)00409-8.

[50] G. W. Lu and H. W. Jun, "Diffusion studies of methotrexate in Carbopol and Poloxamer gels," *Int J Pharm,* Article vol. 160, no. 1, pp. 1-9, 1998, doi: 10.1016/s0378-5173(97)00187-7.

[51] M. L. Marchiori *et al.*, "Hydrogel containing dexamethasone-loaded nanocapsules for cutaneous administration: Preparation, characterization, and in vitro drug release study," *Drug Dev Ind Pharm,* vol. 36, no. 8, pp. 962-71, 2010, doi: 10.3109/03639041003598960.

[52] C. R. Hoffmeister *et al.*, "Hydrogels containing redispersible spray-dried melatonin-loaded nanocapsules: A formulation for transdermal-controlled delivery," *Nanoscale Res Lett,* vol. 7, no. 1, p. 251, 2012, doi: 10.1186/1556-276X-7-251.

[53] M. Reufer *et al.*, "Introducing diffusing wave spectroscopy as a process analytical tool for pharmaceutical emulsion manufacturing," *J Pharm Sci,* vol. 103, no. 12, pp. 3902-3913, 2014, doi: 10.1002/jps.24197.

[54] A. Niederquell, A. H. E. Machado, and M. Kuentz, "A diffusing wave spectroscopy study of pharmaceutical emulsions for physical stability assessment," *Int J Pharm,* vol. 530, no. 1-2, pp. 213-223, 2017, doi: 10.1016/j.ijpharm.2017.07.038.

[55] J. L. Harden and V. Viasnoff, "Recent advances in DWS-based micro-rheology," *Cur Opin Coll Int Sci,* vol. 6, no. 5-6, pp. 438-445, 2001, doi: 10.1016/s1359-0294(01)00115-7.

[56] G. Maret and P. E. Wolf, "Multiple light-scattering from disordered media. The effect of Brownian-motion of scatterers," *Z Phys B Condens Matter,* vol. 65, no. 4, pp. 409-413, 1987, doi: 10.1007/bf01303762.

[57] P. D. Kaplan, M. H. Kao, A. G. Yodh, and D. J. Pine, "Geometric constraints for the design of diffusing-wave spectroscopy experiments," *Appl Opt,* vol. 32, no. 21, pp. 3828-3836, 1993, doi: 10.1364/ao.32.003828.

[58] T. G. Mason, "Estimating the viscoelastic moduli of complex fluids using the generalized Stokes-Einstein equation," *Rheol Acta,* vol. 39, no. 4, pp. 371-378, 2000, doi: 10.1007/s003970000094.

[59] E. M. Furst and T. M. Squires, *Microrheology*, 1st ed. Oxford, UK: Oxford University Press, 2017.

[60] M. Bellour, M. Skouri, J. P. Munch, and P. Hébraud, "Brownian motion of particles embedded in a solution of giant micelles," *Eur Phys J E Soft Matter,* vol. 8, no. 4, pp. 431-6, 2002, doi: 10.1140/epje/i2002-10026-0.

[61] K. Schittkowski, *Numerical data fitting in dynamical systems - A practical introduction with applications and software*, 1 ed. Dordrecht: Kluwer Academic Publisher, 2003.

[62] B. M. Schmidt, S. Allison, and J. S. Wrobel, "Describing normative foot temperatures in patients with diabetes-related peripheral neuropathy," *J Diabetes Sci Technol,* vol. 14, no. 1, pp. 22-27, 2020, doi: 10.1177/1932296819864664.

[63] M. Carabott, C. Formosa, A. Mizzi, N. Papanas, and A. Gatt, "Thermographic characteristics of the diabetic foot with peripheral arterial disease using the angiosome concept," *Exp Clin Endocrinol Diabetes,* vol. 129, no. 2, pp. 93-98, 2021, doi: 10.1055/a-0838-5209.

[64] M. Bharara, J. Schoess, A. Nouvong, and D. G. Armstrong, "Wound inflammatory index: A "proof of concept" study to assess wound healing trajectory," *J Diabetes Sci Technol,* vol. 4, no. 4, pp. 773-9, 2010, doi: 10.1177/193229681000400402.

[65] S. Björklund *et al.*, "The effects of polar excipients Transcutol and dexpanthenol on molecular mobility, permeability, and electrical impedance of the skin barrier," *J Colloid Interface Sci,* vol. 479, pp. 207-220, 2016, doi: 10.1016/j.jcis.2016.06.054.

[66] M. E. Aulton and K. M. G. Taylor, Eds. *Aulton's Pharmaceutics*, 5th ed. Edinburgh, UK: Elsevier Ltd.

[67] C. Loira-Pastoriza, A. Sapin-Minet, R. Diab, J. L. Grossiord, and P. Maincent, "Low molecular weight heparin gels, based on nanoparticles, for topical delivery," *Int J Pharm,* vol. 426, no. 1-2, pp. 256-262, 2012, doi: 10.1016/j.ijpharm.2012.01.044.

[68] J. Li and D. J. Mooney, "Designing hydrogels for controlled drug delivery," *Nat Rev Mater,* vol. 1, no. 12, 2016, doi: 10.1038/natrevmats.2016.71.

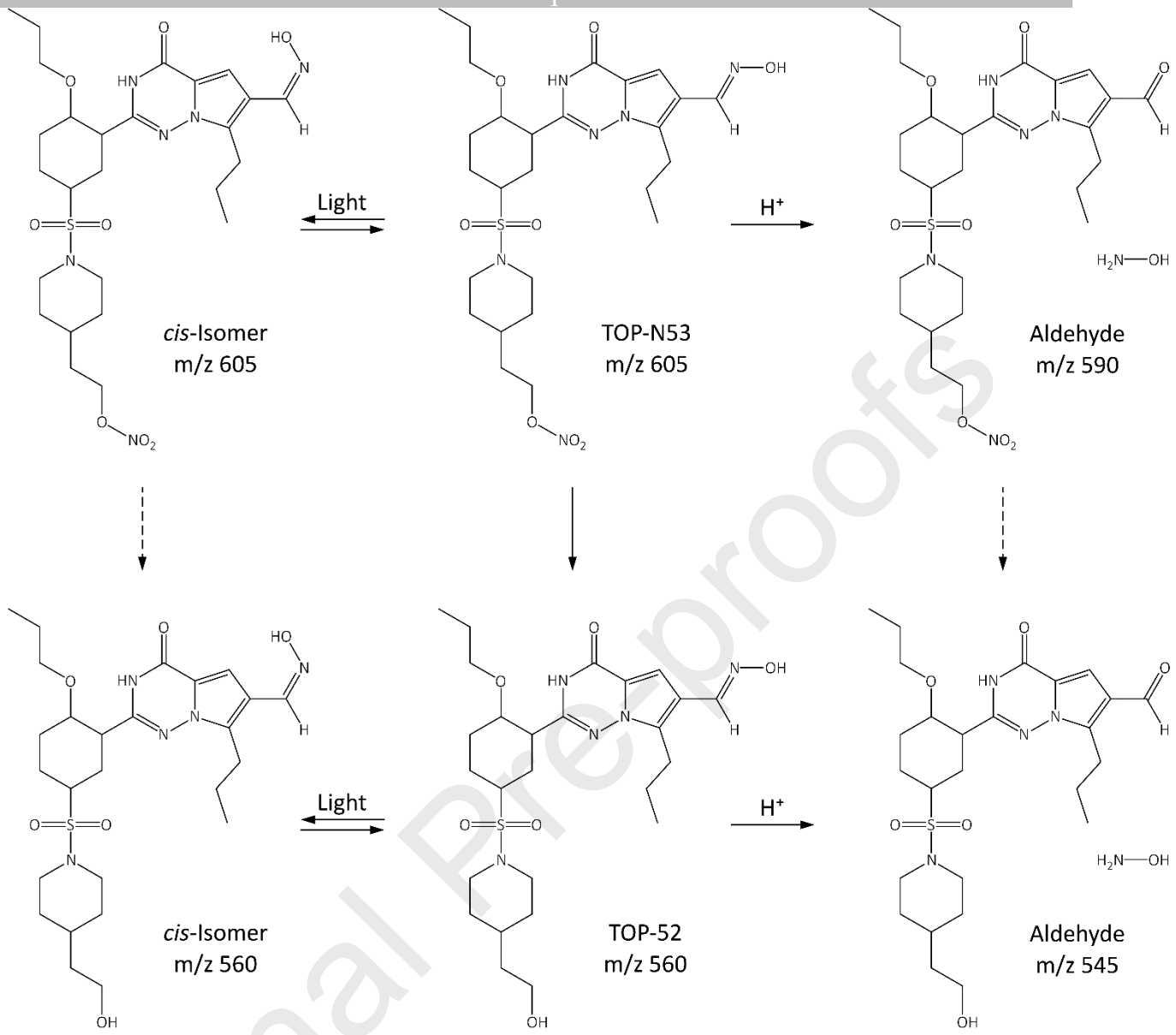

Figure 1: TOP-N53, its metabolite TOP-52 and their chemical degradation products *cis*-isomer and aldehyde. Arrows with solid and dashed lines indicate assumed mechanisms of chemical degradation and metabolism, respectively.

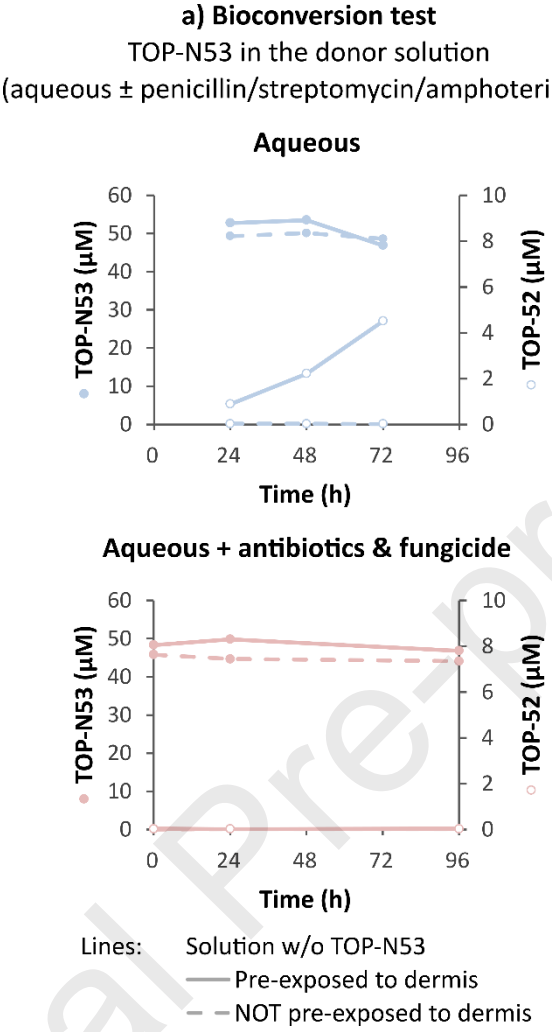

Figure 2a: Effect of bacterial infection on TOP-N53 bioconversion. TOP-N53 (●) and TOP-52 (○) in aqueous (blue, upper graph) and in aqueous vehicle containing antibiotics and fungicide (light red, lower graph). Solid & dashed lines denote pre-exposition and no pre-exposition to dermis, respectively, before addition of TOP-N53 formulation.

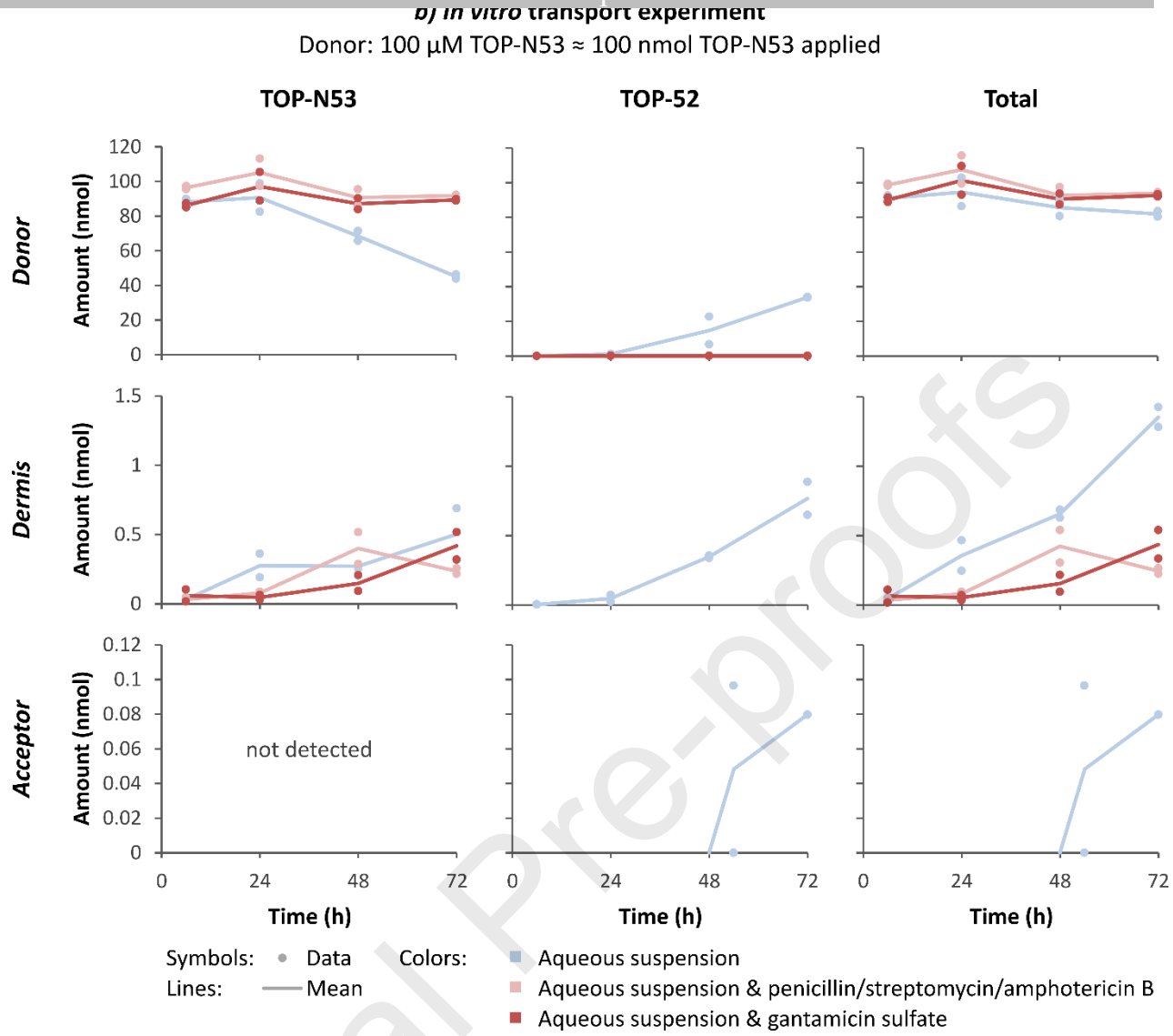

Figure 2b: Effect of bacterial infection on TOP-N53 delivery into the dermis: *In vitro* transport experiment with 100 µM TOP-N53 liquid aqueous suspension formulation. Amount of (from left to right) TOP-N53, TOP-52 and total in (from top to bottom) donor, dermis and acceptor compartment as a function of time. Dots represent data points, lines the mean and colors the presence of antimicrobial agents (blue: No, light & dark red: Penicillin/streptomycin/amphotericin B & gentamicin sulfate, respectively).

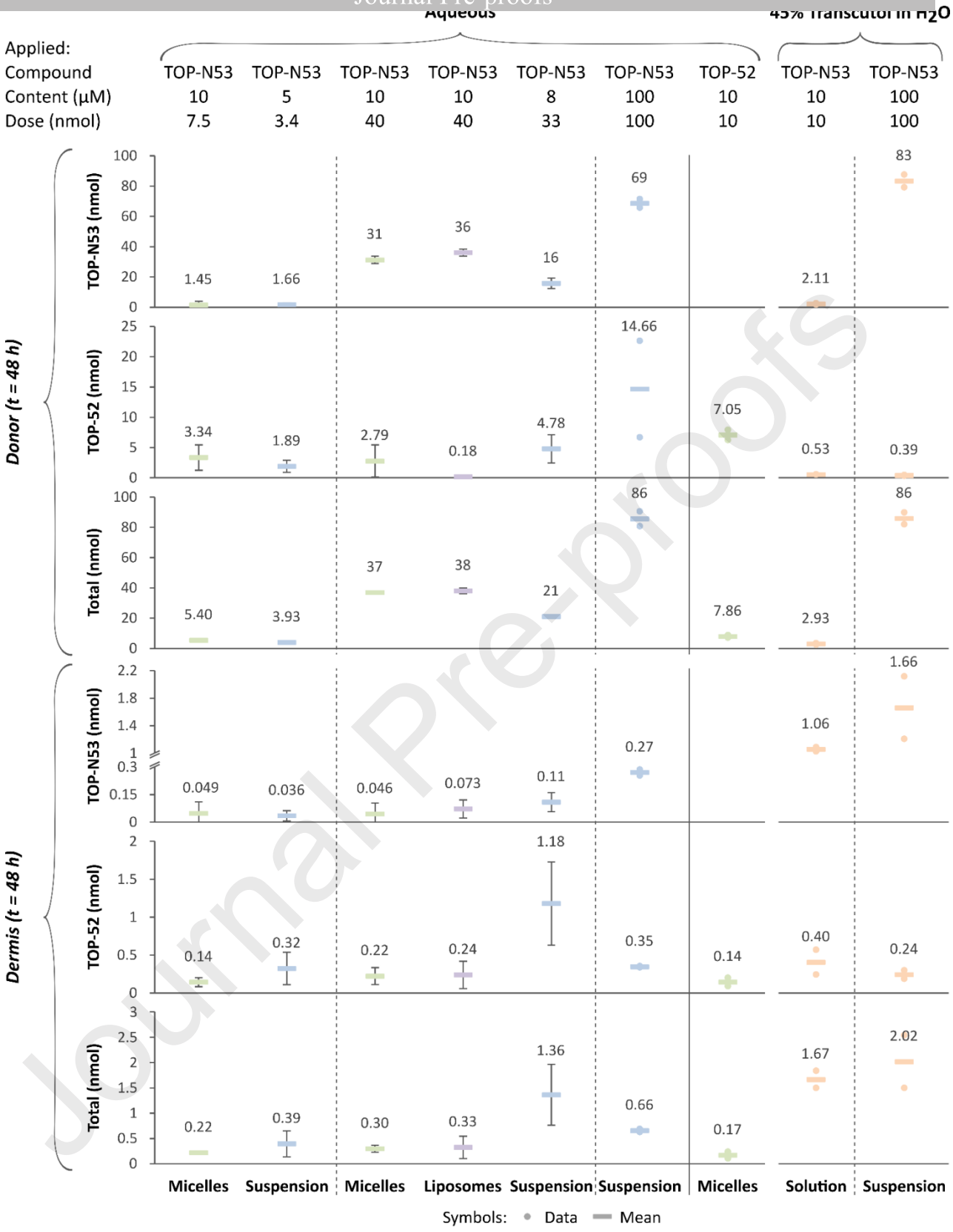

Figure 3: Effect of liquid aqueous and 45% Transcutol in water formulations on TOP-N53 delivery into the dermis: Amount of (from top to bottom) TOP-N53, TOP-52 and total in donor compartment (top 3 graphs) and dermis (bottom 3 graphs) after 48 h (data (●), mean (−) with error bars). Formulations applied: Micellar formulation (micelles), liposomal formulation (liposomes), suspension formulation (suspension) and solution formulation (solution). In the experiment with the micellar formulation with

dose 40 nmol the dermis was pre-treated with microneedles. This pretreatment had no effect on delivery (results not shown).

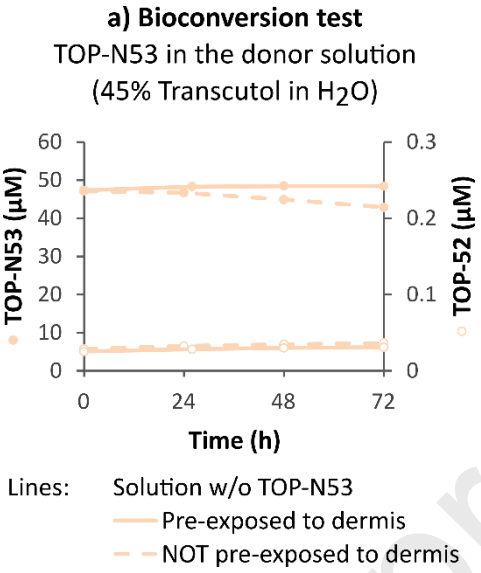

Figure 4a: Effect of Transcutol on bioconversion of TOP-N53 (●) to TOP-52 (○) in 45% Transcutol in water. Solid & dashed lines denote pre-exposition and no pre-exposition to dermis, respectively, before addition of TOP-N53 formulation.

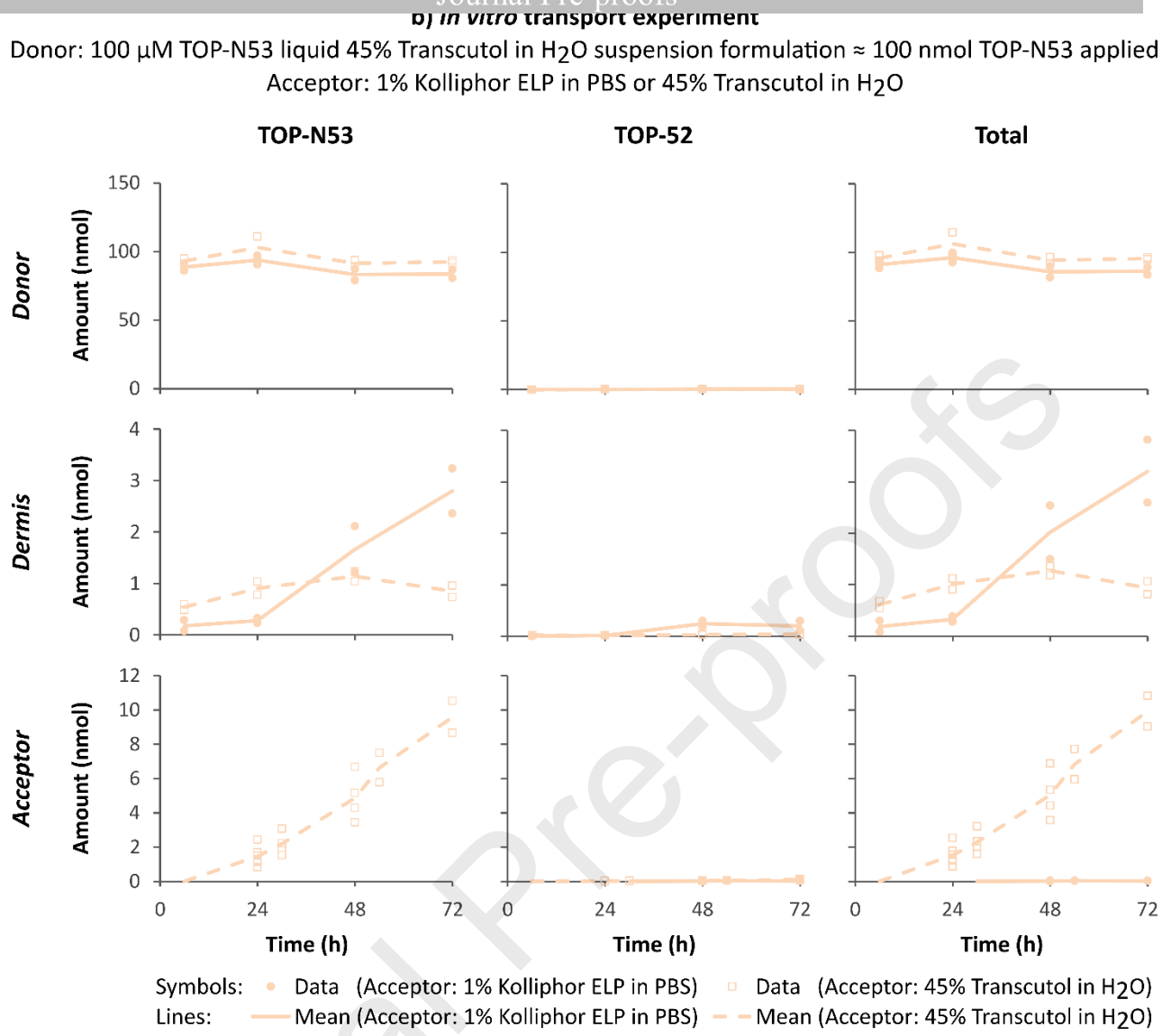

Figure 4b: Effect of Transcutol presence in the acceptor solution on drug transport *In vitro* transport experiment with 100 µM TOP-N53 liquid Transcutol in water suspension formulation: Amount of (from left to right) TOP-N53, TOP-52 and total in (from top to bottom) donor, dermis and acceptor compartment as a function of time. Acceptor solutions: 1% Kolliphor ELP in PBS (Data (●), mean (solid line)) or 45% Transcutol in water (data (□), mean (dashed line)).

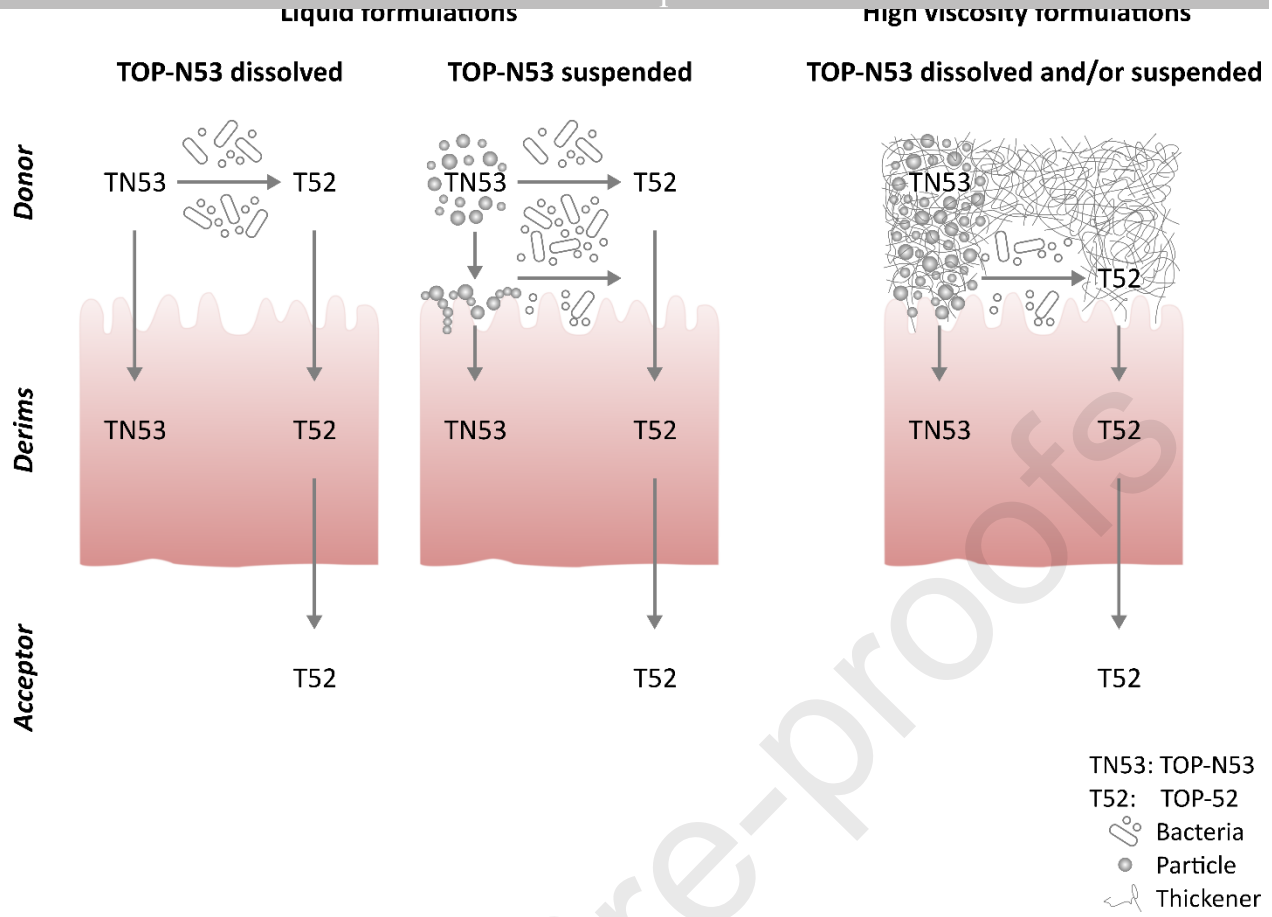

Figure 5: Schematic representation of transport and delivery of TOP-N53 (TN53) and its metabolite TOP-52 (T52) in dermis tissue for different formulations.

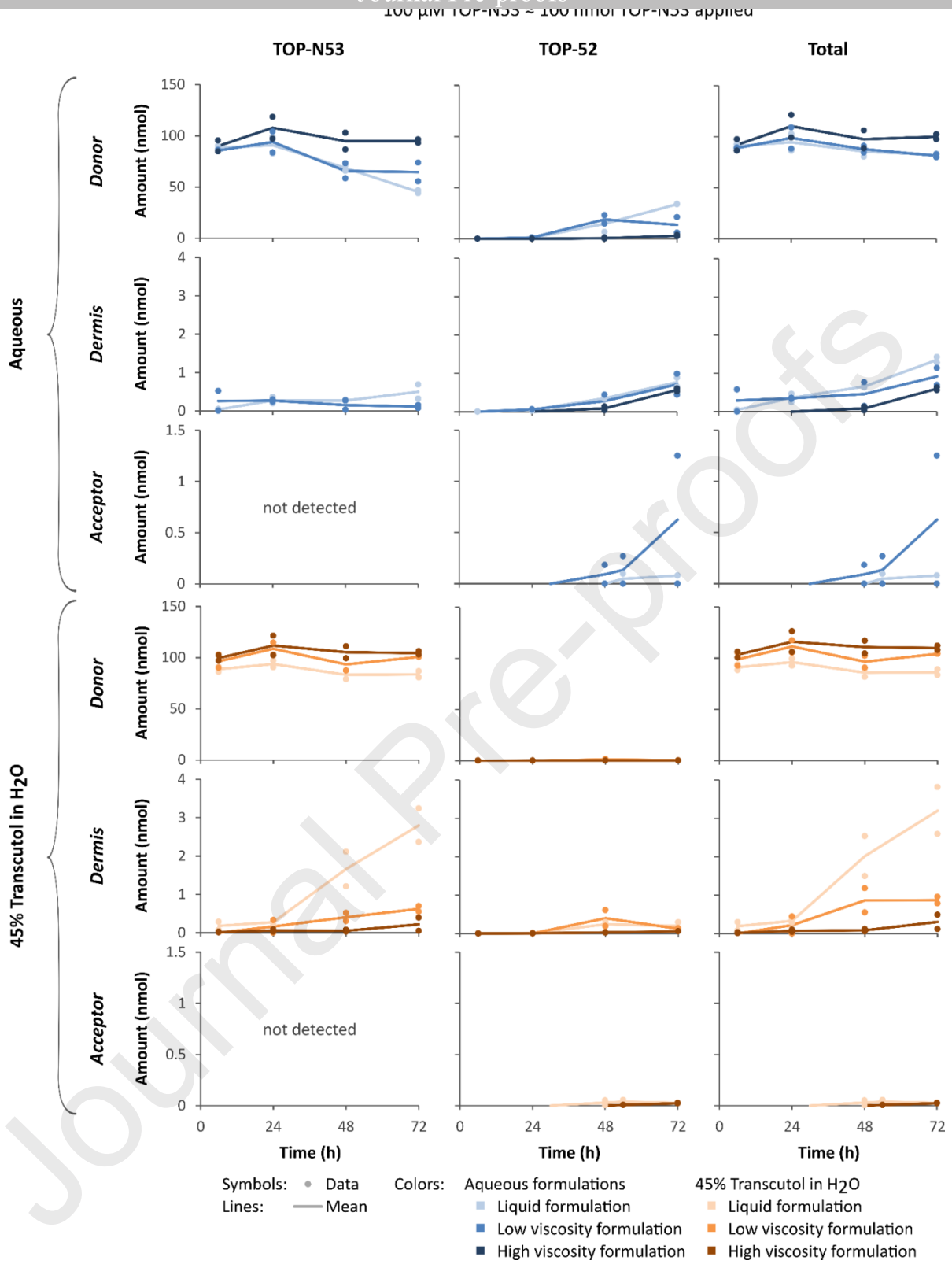

Figure 6: Effect of semisolid suspension formulations on TOP-N53 delivery into the dermis. Amount of (from left to right) TOP-N53, TOP-52 and total in (from top to bottom) donor, dermis and acceptor compartment as a function of time using aqueous (blue, top 3 rows) or 45% Transcutol in water (orange, bottom 3 rows) formulations. Dots represent data points, lines means and intensity in colors viscosity (light to dark: liquid to high viscosity).

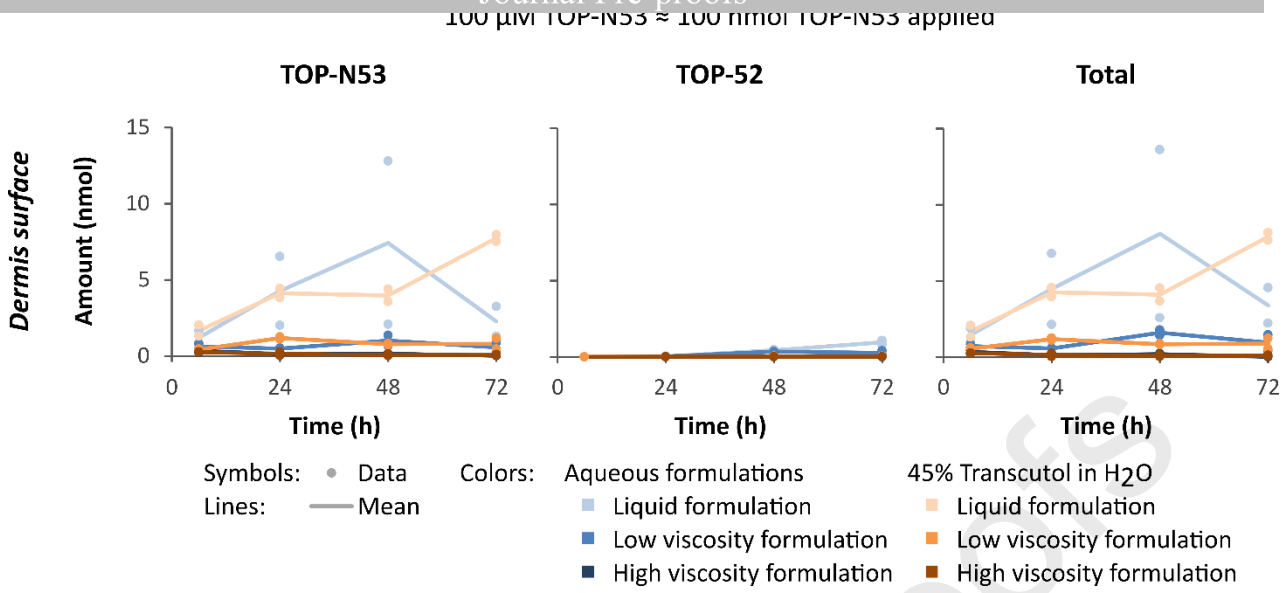

Figure 7: Effect of semisolid suspension formulations on TOP-N53 recovered from the dermis surface. Amount of (from left to right) TOP-N53, TOP-52 and total as a function of time using aqueous (blue) or 45% Transcutol in water (orange) formulations. Dots represent data points, lines means and intensity in colors viscosity (light to dark: liquid to high viscosity).

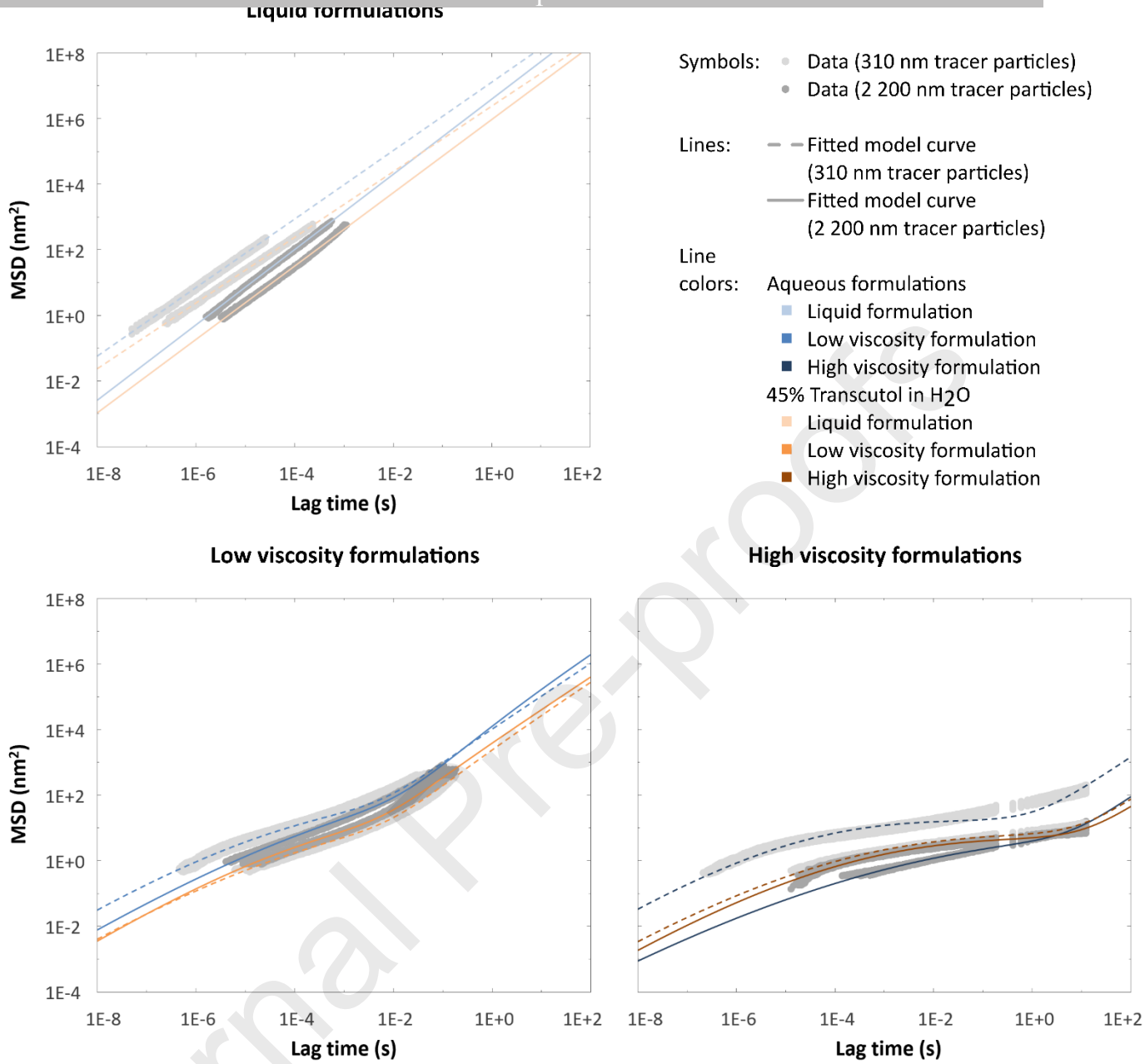

Figure 8: Mean square displacement (MSD) of 310 and 2 200 nm tracer particles in liquid and semisolid suspension formulations: MSD of 310 and 2 200 nm tracer particles in liquid (top left), low viscosity (bottom left) and high viscosity (bottom right) formulation as a function of lag time for aqueous (blue) or 45% Transcutol in H_2O (orange) formulations. Dots represent data points (light grey: 310 nm and dark grey: 2 200 nm tracer particles), lines fitted model curves (dashed: 310 nm and solid: 2 200 nm tracer particles) and intensity in blue and orange colors represents viscosity (light to dark = liquid to high viscosity).

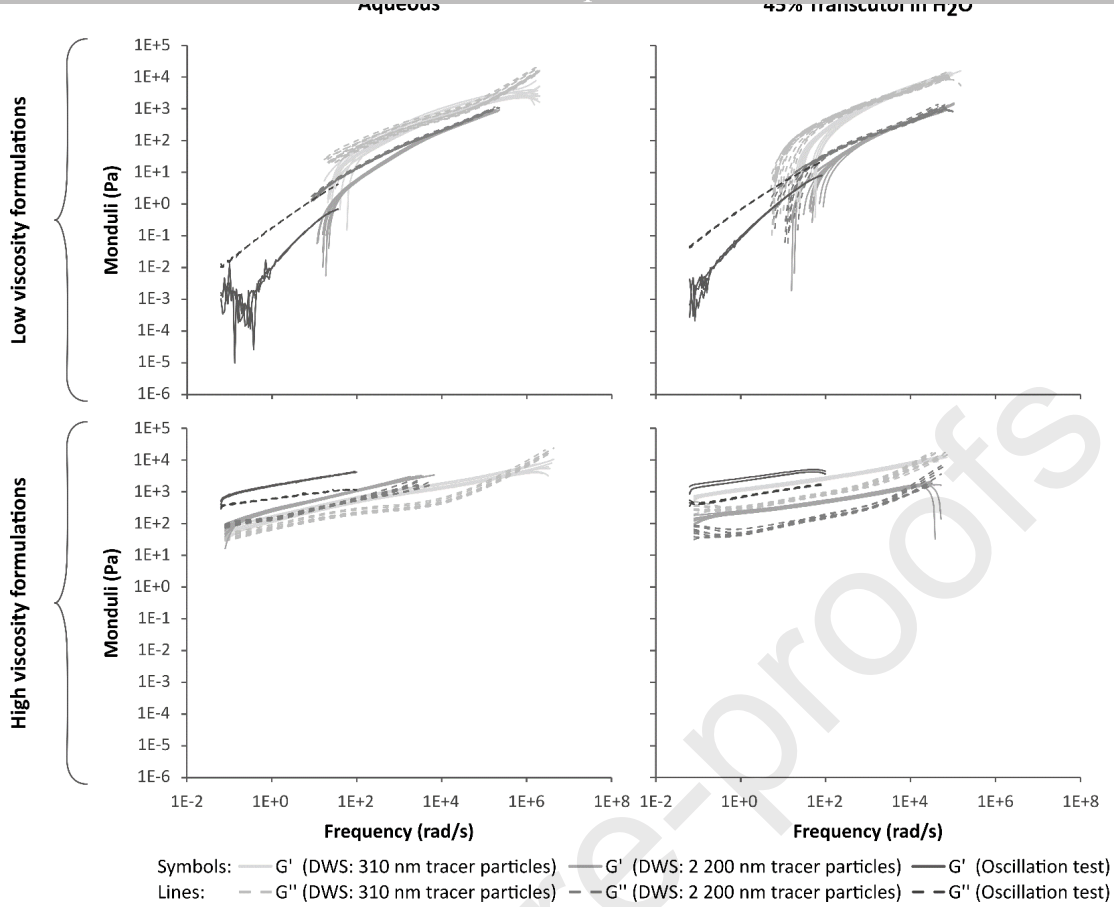

Figure 9: Viscoelastic properties of semisolid formulations: G’ (elastic modulus, solid lines) and G’’ (viscous modulus, dashed lines) of aqueous (left) and 45% Transcutol in water (right) formulations in low (top) and high (bottom) viscosity formulations as a function of frequency. Light and middle colors represent results of DWS measurements (light: 310 nm and middle: 2 200 nm tracer particles) and dark colors of mechanical oscillation tests.

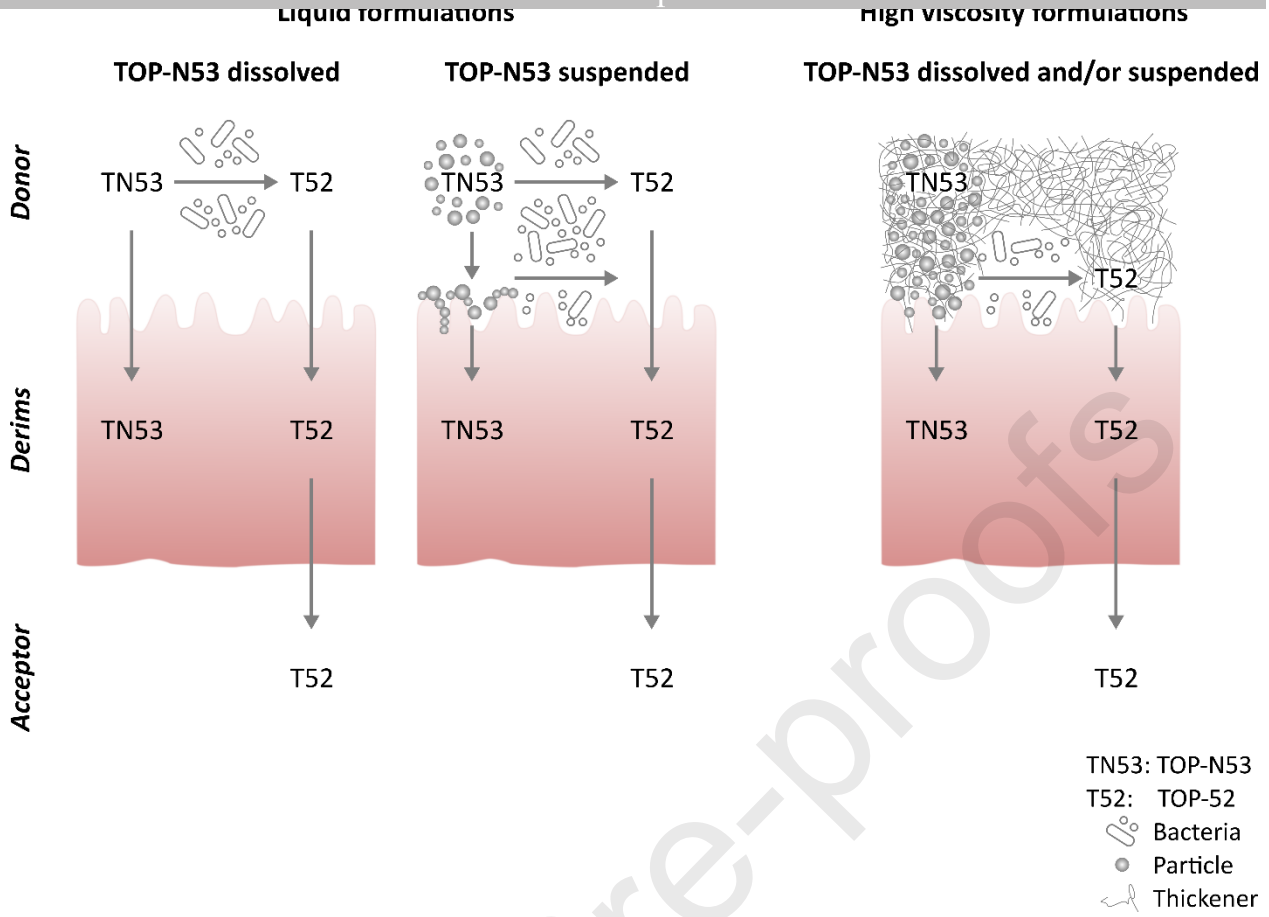

Table 1: Characteristic properties of the liquid formulations (mean values ± SD, n=3).

	Liquid formulations				
Formulations	**Aqueous**			**45% Transcutol in water**	
	Micelles	**Liposomes**	**Suspension**	**Solution**	**Suspension**
Concentration/content (µM)					
– TOP-N53 – TOP-52	10 10	10	5 8 100	10	100
pH	7.3	7.3	7.2	m	7.8

Osmolality (mosmol/kg)	766 ± 0.10	298 ± 1.73	288 ± 1.53	nc
Particle size				
– Z-average (nm)	11.9	124		
– PdI	± 3.96 × 10^{-2}	± 9.64 × 10^{-1}		
– Median x(50%) (µm)	9.16 × 10^{-2} ± 6.84 × 10^{-3}	8.80 × 10^{-2} ± 1.41 × 10^{-2}		
– Distribution width*			2.02 ± 1.0 × 10^{-2} 2.33	3.46 ± 1.0 × 10^{-1} 1.86
Complex viscosity (mPa s)				
at 6 000 rad/s (DWS with 2 200 nm tracer particles)	-	-	1.07 ± 4.78 × 10^{-2}	3.31 ± 1.23 × 10^{-1}

nc: no crystallization, m: missing data, PdI: polydispersity index, *(x(90%)-x(10%))/x(50%)

Table 2: Characteristic properties of the semisolid suspension formulations.

	Semisolid suspension formulations			
Formulations	**Aqueous**		**45% Transcutol in water**	
	Low viscosity	**High viscosity**	**Low viscosity**	**High viscosity**
Content (µM)				
– TOP-N53	100	100	100	100
pH	7.2	5.6	7	m
Osmolality (mosmol/kg)	321 ± 1.00	906 ± 10.12	nc	
Particle size				
– Z-average (nm)				
– PdI				
– Median x(50%) (µm)				
– Distribution width*	2.02	m	2.69	m
	± 6.0×10^{-2}		± 2.0×10^{-2}	
	2.24		1.51	
Complex viscosity (mPa s)				
at 6 000 rad/s (DWS with 2 200 nm tracer particles)	48	987	104	385
	± 2.87	± 218	± 6.89	± 40
Viscoelastic properties				
– Moduli	G’ < G’’	G’ > G’’	G’ < G’’	G’ > G’’

nc: no crystallization, PdI: polydispersity index, m: missing data, G': elastic modulus, G'': viscous modulus.
*(x(90%)-x(10%))/x(50%)

Table 3: ANOVA TOP-N53 & TOP-52 in dermis compartment (t = 72 h) (significant factors are highlighted in bold red).

Data TOP-N53

Transcutol / Viscosity	–	+
Liquid	0.69	3.24
	0.32	2.36
Mean	*0.50*	*2.8*
Low viscosity	0.15	0.69
	0.069	0.55
Mean	*0.11*	*0.62*
High viscosity	0	0.048
	0	0.39
Mean	*0*	*0.22*

ANOVA TOP-N53

Source of variation	Sum of squares (SS)	df	Mean square (MS)	F-ratio	p-value	Critical F-value
Viscosity	5.45	2	2.73	31	**0.000676**	5.14
Transcutol	3.05	1	3.05	35	**0.001048**	5.99
Interaction	2.53	2	1.26	14	**0.00507**	5.14
Error	0.52	6	0.087			
Total	12	11				

Data TOP-52

Transcutol / Viscosity	–	+

ANOVA TOP-52

Source of variation	Sum of squares (SS)	df	Mean square (MS)	F-ratio	p-value	Critical F-value

Liquid	0.65	0.29	**Viscosity**	0.060	2	0.030	0.91	0.450712	5.14
	0.89	0.10	**Transcutol**	0.92	1	0.92	28	**0.001808**	5.99
Mean	*0.77*	*0.20*	**Interaction**	0.0036	2	0.0018	0.056	0.946445	5.14
Low viscosity	0.44	0.14	**Error**	0.20	6	0.033			
	0.98	0.11	**Total**	1.18	11				
Mean	*0.71*	*0.13*							
High viscosity	0.61	0.060							
	0.53	0.059							
Mean	*0.57*	*0.060*							

Table 4: ANOVA TOP-N53 & TOP-52 in donor compartment (t = 72 h) (significant factors are highlighted in bold red).

Data TOP-N53

Transcutol / Viscosity	−	+
Liquid	47	87
	44	81
Mean	*45*	*84*
Low viscosity	74	101
	55	101
Mean	*65*	*101*
High viscosity	93	103
	96	106
Mean	*95*	*105*

ANOVA TOP-N53

Source of variation	Sum of squares (SS)	df	Mean square (MS)	F-ratio	p-value	Critical F-value
Viscosity	2 483	2	1242	37	**0.000433**	5.14
Transcutol	2 387	1	2387	70	**0.000156**	5.99
Interaction	510	2	255	7.53	**0.023158**	5.14
Error	203	6	34			
Total	5 583	11				

Data TOP-52

Transcutol / Viscosity	−	+

ANOVA TOP-52

Source of variation	Sum of squares (SS)	df	Mean square (MS)	F-ratio	p-value	Critical F-value

Liquid	34	0.27	**Viscosity**	488	2	244	13	**0.007216**	5.14
	34	0.19	**Transcutol**	824	1	824	42	**0.00063**	5.99
Mean	*34*	*0.23*	**Interaction**	491	2	245	13	**0.00713**	5.14
Low viscosity	6.02	0.46	**Error**	117	6	19			
	21	0.32	**Total**	1 920	11				
Mean	*14*	*0.39*							
High viscosity	2.50	0.27							
	3.65	0.21							
Mean	*3.08*	*0.24*							

Table 5: Estimated parameter values ± standard error (n = 9-15) of Eq. 1 and Eq. 2 for liquid, low and high viscosity aqueous and 45% Transcutol in water formulations.

Formulation		Tracer (nm)	D_0 (nm²/s)	Dm (nm²/s)	δ^2 (nm²)	x	α
Aqueous	Liquid	310	2 179 805 ± 7.01 × 10^{-12}			1.05 ± 2.07 × 10^{-04}	
		2 200	661 282 ± 2.61 × 10^{-11}			1.15 ± 1.84 × 10^{-04}	
	Low viscosity	310	2 179 805*	1 742 ± 35	11 ± 3.94 × 10^{-1}		0.14 ± 1.17 × 10^{-3}
		2 200	661 282*	3 397 ± 112	46 ± 2.05		0.11 ± 7.50 × 10^{-4}
	High viscosity	310	2 179 809*	2.40 ± 3.65 × 10^{-2}	2.78 ± 3.26 × 10^{-2}		0.16 ± 1.04 × 10^{-3}
		2 200	661 282*	0.17 ± 1.73 × 10^{-3}	1.16 ± 1.90 × 10^{-2}		0.081 ± 2.98 × 10^{-4}
45% Transcutol in water	Liquid	310	404 738 ± 3.39 × 10^{-11}			1.00 ± 1.64 × 10^{-04}	
		2 200	157 962			1.12	

		± 2.01 × 10^{-10}				± 3.16 × 10^{-04}
Low viscosity	**310**	404 738*	459 ± 14	4.03 × 10^{-1}	± 2.12	0.12 ± 1.26 × 10^{-3}
	2 200	157 962*	675 ± 15	4.66 ± 2.27 × 10^{-1}		0.15 ± 1.68 × 10^{-3}
High viscosity	**310**	404 738*	0.12 ± 1.85 × 10^{-3}	1.08 ± 7.45 × 10^{-3}		0.12 ± 3.58 × 10^{-4}
	2 200	157 962*	0.068 ± 1.58 × 10^{-3}	0.82 ± 6.57 × 10^{-3}		0.13 ± 4.58 × 10^{-4}

*fixed values